

SUBCRITICAL FLOW PAST SLENDER BODIES BY A TRANSONIC INTEGRAL EQUATION METHOD

**A Thesis Submitted
In Partial Fulfilment of the Requirements
for the Degree of
MASTER OF TECHNOLOGY**

**By
J. P. AGARWAL**

**to the
DEPARTMENT OF AERONAUTICAL ENGINEERING
INDIAN INSTITUTE OF TECHNOLOGY, KANPUR
SEPTEMBER, 1979**

CERTIFICATE

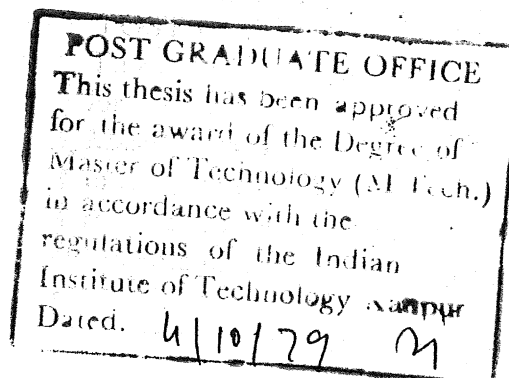
This is to certify that the work ' SUBCRITICAL FLOW
PAST SLENDER BODIES BY A TRANSONIC INTEGRAL EQUATION METHOD'
has been carried out under my supervision and has not been
submitted elsewhere for a degree.

September, 1979.

NLA^{ms}

(N. L. ARORA)
Professor

Department of Aeronautical Engineering
Indian Institute of Technology, Kanpur.



A C K N O W L E D G E M E N T S

I express my sincere thanks to Dr. N. L. Arora for his guidance and encouragement.

I thank Mr. S.S. Pethkar for his accurate typing and Mr. Tiwari for cyclostyling.

Finally, I wish to express my indebtedness to my friends who helped me a lot at different stages of the work.

September 1979.

J. P. AGARWAL

TABLE OF CONTENTS

	Page
ABSTRACT	iii
LIST OF SYMBOLS	iv
LIST OF FIGURES	vi
 CHAPTER 1 INTRODUCTION	
1.1 General	1
1.2 Literature Survey	3
1.3 Present work	7
 CHAPTER 2 PROBLEM SPECIFICATION	
2.1 Introduction	8
2.2 Axisymmetric flow	8
2.3 Two-dimensional flow.	12
 CHAPTER 3 INTEGRAL EQUATION METHOD OF SOLUTION	
3.1 Introduction	14
3.2 Axisymmetric flow	14
3.2.1 Volume integral	17
3.2.2 Surface integral	18
3.3 Two-dimensional flow	23
3.3.1 Surface integral	26
3.3.2 Line integral	27
 CHAPTER 4 NUMERICAL SCHEME	
4.1 Introduction	31
4.2 Axisymmetric flow	31
4.3 Two-dimensional flow	36
 CHAPTER 5 RESULTS AND DISCUSSION	
5.1 Introduction	40
5.2 Axisymmetric flow	40
5.3 Two-dimensional flow	43
5.4 Conclusion.	44

REFERENCES	45
APPENDIX A	48
APPENDIX B	51
APPENDIX C	53
APPENDIX D	55
APPENDIX E	58
APPENDIX F	

ABSTRACT

The subcritical transonic flow past axisymmetric and two-dimensional slender bodies has been studied in the present work. The integral equation approach has been adopted. For this nonlinear transonic small disturbance equation is transformed into an integral equation using Green's theorem. The solution for the axial perturbation velocity at a general point in the flow field is sought in the meridian plane by dividing the region of integration into rectangular elements, wherein the axial perturbation velocity is taken uniform. Thus an iterative scheme is developed of which convergence is sought. The results are computed for a parabolic arc of revolution, parabolic airfoil and NACA-0012 airfoil. The results obtained are compared with experimental results and/or results obtained by advanced relaxation methods.

LIST OF SYMBOLS

C_p	Pressure coefficient
E	Complete elliptic integral of second kind
F	Complete elliptic integral of second kind
FR	Fineness ratio of parabolic arc of revolution
(h/c)	tunnel half height to body : chord ratio.
L	Laplacian operator
M	Mach number
p	Porosity parameter
x, r, θ	Normalised cylindrical co-ordinates
$\bar{x}, \bar{r}, \bar{\theta}$	Transformed cylindrical co-ordinates
x, y, z	Normalised cartesian co-ordinates
$\bar{x}, \bar{y}, \bar{z}$	Transformed cartesian co-ordinates
γ	Ratio of specific heats (= 1.4 for air)
ξ, ρ, ν	Running co-ordinates in $\bar{x}, \bar{r}, \bar{\theta}$ directions.
ξ, ζ	Running coordinates in \bar{x}, \bar{y} directions.
\bar{u}	Perturbation velocity in \bar{x} -direction.
\bar{u}_L	Linear perturbation velocity
τ	Thickness ratio
ϕ	Perturbation velocity potential
$\bar{\phi}$	Transformed perturbation velocity potential
ψ	Parameter satisfying Laplace equation

Subscripts

y

i, j	Values of variable at different locations
x, r, θ	Partial derivative of variable w.r.t. x, r, θ
$\bar{x}, \bar{r}, \bar{\theta}$	Partial derivative of variable w.r.t. $\bar{x}, \bar{r}, \bar{\theta}$
x, y, z	Partial derivative of variable w.r.t. x, y, z
$\bar{x}, \bar{y}, \bar{z}$	Partial derivative of variable w.r.t. $\bar{x}, \bar{y}, \bar{z}$
ξ, ρ, ν	Partial derivative of variable w.r.t. ξ, ρ, ν
ξ, ζ	Partial derivative of variable w.r.t. ξ, ζ
∞	Free stream condition.

LIST OF FIGURES

1. Slender body in axisymmetric flow.
2. Thin airfoil in two-dimensional flow.
3. Location of grid point in rectangular elements .
(axisymmetric flow) .
4. Location of grid points in rectangular elements .
(two dimensional flow) .
5. Distribution of C_p on parabolic arc of revolution
($M_\infty = 0.9$, $FR = 10$, Free air case) .
6. Distribution of C_p for parabolic arc of revolution.
($M_\infty = 0.9$, $FR = 10$, Free air case) .
7. Distribution of C_p for parabolic arc of revolution.
($M_\infty = 0.9$, $FR = 10$) wall interference case with
porosity parameter 0.77 and wall radius 1.17.
8. Distribution of C_p on parabolic arc of revolution
($M_\infty = 0.85$, $FR = 10$, wall radius 1.17) .
9. Distribution of C_p on parabolic arc of revolution
($M_\infty = 0.9$, $FR = 10$, Solid wall at 1.17) .
10. Distribution of C_p on parabolic arc of revolution
($M_\infty = .9$, $FR = 10$, wall at 1.17) .
11. Distribution of C_p on parabolic arc of revolution in
free air at supercritical shock free mach numbers ($FR = 10$) .
12. Distribution of C_p on general parabolic body of revolution
in free air ($M_\infty = 0.9$, $FR = 10$) .

13. Distribution of C_p on NACA-0012 airfoil at zero incidence in free air ($M_\infty = 0.72$).
14. Distribution of C_p on 6 percent thick parabolic airfoil at zero incidence ($M_\infty = 0.825$)
15. Distribution of C_p on 6 percent thick parabolic airfoil at zero incidence with wall interference. ($M_\infty = 0.825$, $h/c = 2.0$).
16. Distribution of C_p on 6 percent thick parabolic airfoil at zero incidence at Mach number 0.7 and 0.8 in free air by present method.

CHAPTER 1

INTRODUCTION

1.1 General :

Despite much advances in aerodynamic research for flight regime lying far beyond the so called sonic barrier, there still remains some problems connected with the phenomenon that occur in the flight range straddling the speed of sound. Consequently this range - transonic flow range - continues to engage substantial research effort and gained impetus due to possible development of minimum drag transonic cruise configuration for transport aircraft

To simplify the study of transonic flow and for ease of building the mathematical model, following assumptions are made :

- i) the fluid is ideal and perfect gas ;
- ii) the medium is continuum and homogeneous;
- iii) the flow is steady and irrotational
- and iv) the body considered is slender.

Under these conditions with perturbation velocity (ϕ_x, ϕ_y, ϕ_z) being quite small the equation for perturbation velocity potential is given by Prandtl-Glauert equation :

$$(1 - M_{\infty}^2) \phi_{xx} + \phi_{yy} + \phi_{zz} = 0$$

The above equation governs subsonic and supersonic flow quite reasonably. However since in the transonic range $M_\infty \rightarrow 1$ the coefficient of ϕ_{xx} on L.H.S. becomes very small hence an order of magnitude analysis of gas dynamics equation necessitates retention of some non-linear terms also. The final equation takes the form²⁷:

$$(1 - M_\infty^2) \phi_{xx} + \phi_{yy} + \phi_{zz} = M_\infty^2 (\gamma + 1) \phi_x \phi_{xx}$$

The above equation in cylindrical co-ordinates is :

$$(1 - M_\infty^2) \phi_{xx} + \phi_{rr} + \frac{1}{r^2} \phi_{\theta\theta} + \frac{1}{r} \phi_r = M_\infty^2 (\gamma + 1) \phi_x \phi_{xx}$$

This small perturbation equation is equally valid for transonic, subsonic and supersonic flows. In the x-r plane, it is a mixed hyperbolic parabolic and elliptic type nonlinear equation i.e. for :

$$\left[1 - M_\infty^2 - M_\infty^2 (\gamma + 1) \phi_x \right] \begin{cases} > 0 & \text{elliptic (subcritical flow)} \\ = 0 & \text{parabolic (critical flow)} \\ < 0 & \text{hyperbolic (supercritical flow)} \end{cases}$$

The shock free supercritical case is of particular interest as it gives minimum drag for the body.

To solve the transonic flow equation many methods have been tried of which relaxation method is quite standard method but needs a lot of labour. An equally good technique is integral equation approach. It is less time consuming and attempts are being made to make it of similar accuracy

as that of relaxation method. A brief survey of integral equation method is presented in the following section.

1.2 Literature Survey :

Integral equation approach is one of the earliest successful method for solving the direct transonic flow problem. The main idea is to convert the transonic flow equation into an integral equation using Green's Theorem. The solution to the integral equation is obtained by iterative technique after certain modifications have been incorporated into the equation so obtained.

Among the most noteworthy earliest attempts for the solution of transonic flow problem by integral equation method are three related studies that deserve special mention. These include those carried out by Oswatitsch, Gullstrand and Spreiter and Alksne, and hence the approach adopted has been termed as OGSA approach by Ferrari¹. Oswatitsch² deduced a non-linear integral equation over the whole plane flow at zero lift and made approximate calculations for some aerofoil in the lower transonic range. The work was later extended and illustrated with applications by Gullstrand³⁻⁷. The more recent exposition of the method is given by Spreiter and Alksne⁸, who worked out the method more thoroughly. Their results are fairly good for the

subcritical flow around circular arc airfoil at zero incidence. Heaslet and Spreiter⁹ applied the integral equation method to transonic flow around slender wing and bodies of revolution. Special attention was given to conditions resulting from shock waves. Results are obtained for cone cylinders, wings and wing body combinations at a free stream Mach no. = 1 and compared with experimental results.

Nørstrød¹⁰⁻¹³ extended the OGSA integral equation method to lifting and non-lifting transonic flow problems, including the flow with shock discontinuities. The integral equation is transformed into a set of non-linear algebraic equations. To ensure a unique solution for supercritical shock free flows the method of parametric differentiation has been applied. His results indicate generally good agreement with experimental results and otherwise accurate results like ^{those} obtained by finite difference techniques.

The integral equation method to solve the problem of high subsonic flow past a steady two-dimensional airfoil has also been used by Nixon and Hancock¹⁴. They have computed the shock free two-dimensional flows around the lifting and non-lifting airfoils by solving the integral equations approximately. The results for two test cases show close agreement with more exact numerical results of Sells¹⁸.

The method has also been extended by Nixon¹⁵ to an airfoil oscillating at low frequency in high subsonic flow.

A feature common to all above integral equation methods is that the field integral is not evaluated accurately. In these methods using a functional relationship for velocity distribution, the double (surface) integral is reduced to a line integral in the plane of the airfoil. In the extended integral equation method of Nixon¹⁶ an alternative means of evaluating the field integral is developed. The flow field is divided into a number of streamwise strips and the transverse variation of perturbation velocities across each of these strips is approximated by an interpolation function in terms of values on the strip edges. The field integral is then reduced to a line integral which is in turn evaluated by quadrature. The results obtained by using this method have been compared with those of the standard integral equation method (See Nixon¹⁷). It is shown that this method gives considerably improved results over the earlier integral equation methods.

Recently Ogana¹⁹ obtained results for two-dimensional parabolic arc airfoil evaluating the field integral quite accurately. He divided the region of integration into closed rectangular elements, and considered velocity to be constant in each element; the integral equation is then reduced

to matrix equation solvable by suitable iterative scheme for subcritical flows.

The influence of wall interference effects on models tested in transonic wind tunnels has been an open question for many years. There has been an increasing need for the largest model possible. The relaxation method has been applied to the problem of wall interference effects. Bailey²⁰ treated the slender bodies of revolution at transonic speeds in the presence of wind-tunnel wall boundaries, while Murman²¹ and Kaoprzynski²² have considered interference effects on two-dimensional airfoil. Newman and Klucker²³ have extended relaxation method to determine interference effects of transonic flow over finite lifting wings in rectangular tunnels. Murman, Bailey and Johnson²⁴ have given an up to date computer program to solve the transonic small disturbance equation for two dimensional flow for lifting airfoil which takes free air case as well as various wind tunnel wall conditions. They used finite difference formulation using iterative successive line over relaxation (SIOR) algorithm. An integral equation method has also been used by Krafft²⁵ for wind tunnel boundary interference at transonic speeds on thin airfoil in two-dimensional wind tunnels. However, field integral is reduced to a line integral over the airfoil by the use of arbitrary approximate function and the results are obtained on an airfoil.

1.3 Present Work :

The integral equation method applied to two-dimensional flow has proved to give good results. However, the attempts to solve the problem of mixed transonic flow past bodies of revolution by integral equation method have been dismal.

In present work an integral equation suitable for axisymmetric flow past slender bodies of revolution at transonic speeds is obtained in the free air and in the presence of porous wall boundaries. The numerical solution to integral equation is sought in the meridian plane by dividing the region of integration into rectangular elements wherein the velocity can be considered uniform. The pressure field is computed on and away from the slender body including force and aft body effects. An application to parabolic bodies of revolution with and without sting is presented at subsonic Mach numbers yielding subcritical and slightly supercritical shock free flows.

Similar analysis has been carried out for two-dimensional flows also. Parabolic airfoil has been considered in the free air and in the presence of porous wall. An attempt is also made to determine pressure field for NACA 0012 airfoil at zero incidence.

CHAPTER 2

PROBLEM SPECIFICATION

2.1 Introduction:

Most of the aerodynamic problems are related with finding pressure field over two-dimensional or axisymmetric bodies, so that one can predict coefficients of lift, drag or moment over a body in certain situations. Here we are interested in finding pressure field on and away from body. The axisymmetric problem is considered first and then the flow past two dimensional non lifting airfoil is treated.

2.2 Axisymmetric Flow :

Consider the inviscid, compressible flow about a slender, pointed body of revolution in cylindrical coordinates x and r (made dimensionless with respect to the length of the body) with x axis parallel to the body axis and free stream velocity U_∞ (see fig. 1). Assume shock free flow so there is no vorticity involved. Under this assumption a velocity potential can be used to calculate the flow field. In particular a perturbation potential can be defined such that the perturbation velocities, made dimensionless with respect to the free stream velocity, are $u = \phi_x$ parallel to the x -axis and $v = \phi_r$ parallel to r -axis.

The governing differential equation for transonic flow given by slender body theory can be written as²⁷

$$(1 - M_\infty^2) \phi_{xx} + \phi_{rr} + \frac{1}{r} \phi_r = (\gamma + 1) M_\infty^2 \phi_x \cdot \phi_{xx} \quad (2.1)$$

where M_∞ is free stream mach number and γ is the ratio of specific heats.

The term associated with ϕ_x makes transonic equation both nonlinear and of mixed elliptic-hyperbolic type. The mixed character of the flow field here may occur with local supersonic regions embedded in a subsonic flow.

To complete the specification of problem, boundary conditions must be given at the body and in the outer flow. The flow tangency condition at the body surface given by the first-order slender body approximation is that near the body axis²⁷:

$$\begin{aligned} \lim_{r \rightarrow 0} r \phi_r &= R \frac{dR}{dx} \\ &= \frac{S'(x)}{2\pi} \end{aligned} \quad (2.2)$$

where $r = R(x)$ defines body

$S(x)$ defines cross sectional area of the body and

$'$ prime denotes derivative of function w.r.t. its argument.

For a body in free air the perturbation velocities

vanish at infinity:

$$\phi_x, \phi_r \rightarrow 0 \text{ as } \sqrt{x^2 + r^2} \rightarrow \infty \quad (2.3)$$

which is satisfied by setting ϕ equals a constant, say zero, at infinity.

In addition to the free air boundary condition wall boundary condition may be given to approximate inviscid flow in porous wall wind tunnel test sections. These boundary conditions can be used to illustrate wall-induced interference effects. Although the formulation is strictly valid for a circular test section, the results may be compared with a square test section of equal cross sectional area because the effects of wall interference at the centre of tunnel should be relatively insensitive to the actual wall shape.

The average boundary condition for a porous wall, as derived by Goodman²⁶ follows from Darcy's law for slow viscous flow through a porous medium. It is assumed that the average velocity normal to the wall is proportional to the pressure difference across the wall, which is a linearized approximation of Darcy's law for a thin wall, and pressure outside the wall is free stream pressure. With the wall parallel to x-axis the porous wall boundary condition becomes:

$$\phi_r + p\phi_x = 0 \text{ at the wall } r = r_w \quad (2.4)$$

The quantity p is a porosity parameter or Reynolds Number of the porous medium, defined by :

$$p = \frac{U_{\infty} \rho_{\infty} k}{\mu t} \quad (2.5)$$

where

U_{∞} free stream velocity

ρ_{∞} free stream density

k permeability of porous medium

μ viscosity of air

t tunnel wall thickness

k is determined by the structure of the porous medium and must be found experimentally²⁶.

As porosity parameter vanishes i.e. $p = 0$ equation (2.4) gives boundary condition for solid wall and the porosity parameter becomes very large i.e. $p \rightarrow \infty$ equation (2.4) approaches the open jet boundary. Although truly porous walls are seldom used for transonic wind tunnels, the porous wall approximation is useful mean boundary condition for perforated walls.

Finally, the slender body approximation for the pressure coefficient at points near the body is given by²⁷

$$C_p = -2\phi_x - \phi_r^2 \quad (2.6)$$

and on the body surface

$$C_p = -2\phi_x - (dR/dx)^2 \quad (2.7)$$

1.3 Two-Dimensional Flow :

Here Cartesian coordinates (made dimensionless w.r.t. the length of airfoil) has been chosen to describe the inviscid, compressible, shock free flow over a thin symmetric airfoil. The x-axis has been taken to be parallel to airfoil plane and the free stream velocity U_∞ (see fig.2). The perturbation velocities made dimensionless w.r.t. the free stream velocity U_∞ , are $u = \phi_x$ parallel to the x-axis and $v = \phi_y$ parallel to the y-axis.

The governing equation for transonic flow given by thin airfoil theory can be written as²⁷

$$(1 - M_\infty^2) \phi_{xx} + \phi_{yy} = (\gamma + 1) M_\infty^2 \phi_x \phi_{xx} \quad (2.8)$$

where symbols have same meaning as in previous section:

The boundary condition for thin airfoil is given by²⁷

$$\lim_{y \rightarrow \pm 0} \phi_y(x, \pm 0) = \frac{dY_{\pm}}{dx} \quad (2.9)$$

where $y = \begin{cases} Y_+(x) & \text{defines upper airfoil profile} \\ Y_-(x) & \text{defines lower airfoil profile} \end{cases}$

For symmetric airfoil $Y_+(x) = -Y_-(x)$.

For the airfoil in free air perturbation velocity vanish at infinity which is satisfied by setting

$$\phi_x, \phi_y \rightarrow 0 \text{ as } \sqrt{x^2 + y^2} \rightarrow \infty \quad (2.10)$$

For wall interference case the effect of porous wall, parallel to free stream can be taken by applying porous wall boundary condition given by²⁶

$$\phi_y \pm p \phi_x = 0 \quad \text{at } y = \pm y_w$$

where + sign is for upper wall, - sign is for lower wall, and p is defined by (2.5).

The thin airfoil approximation for pressure coefficient for the point near the airfoil is given by

$$C_p = 2/\gamma M_\infty^2 \left\{ \left[1 + \frac{\gamma-1}{2} M_\infty^2 (1 - (\pm \phi_x)^2 - \phi_y^2) \right]^{\gamma/(\gamma-1)} - 1 \right\} \quad (2.12)$$

CHAPTER 3

INTEGRAL EQUATION METHOD OF SOLUTION

3.1 Introduction:

In this chapter the governing nonlinear partial differential equation of transonic flow is transformed into an integral equation using Green's Theorem for subcritical and shock free supercritical speeds ($M_\infty < 1$). Axisymmetric and non-lifting two dimensional cases have been dealt with. The axisymmetric case will be treated first.

3.2 Axisymmetric flow:

To apply the Green's Theorem to the axisymmetric transonic flow equation (2.1) one stretches the coordinate system suitably. Here we make the following transformations:

$$\bar{x} = x ; \quad \bar{r} = \beta r ; \quad \bar{\phi} = \frac{K}{\beta^2} \phi \quad (3.1)$$

where $\beta = \sqrt{1 - M_\infty^2}$

$$K = [\gamma + 1] M_\infty^2$$

Now the governing transonic flow equation for axisymmetric flow (eq. 2.1) can be expressed as

$$\bar{\phi}_{\bar{x}\bar{x}} + \bar{\phi}_{\bar{r}\bar{r}} + \frac{1}{\bar{r}} \bar{\phi}_{\bar{r}} = \bar{\phi}_{\bar{x}} \bar{\phi}_{\bar{x}\bar{x}} \quad (3.2)$$

Similarly boundary conditions equations (2.2), (2.3) and (2.4) become

$$\lim_{\bar{r} \rightarrow 0} \bar{r} \bar{\phi}_{\bar{r}} = \frac{K}{\beta^2} \frac{S'(\bar{x})}{2\pi} \quad (3.3)$$

$$\bar{\phi}_{\bar{x}}, \bar{\phi}_{\bar{r}} \rightarrow 0 \quad \text{at infinity} \quad (3.4)$$

and for wall interference case at the wall $\bar{r} = \bar{r}_w$:

$$\bar{\phi}_{\bar{r}} + p/\beta \bar{\phi}_{\bar{x}} = 0 \quad (3.5)$$

Now we shall apply Green's Theorem to the equation (3.2).

The theorem states that the following relation holds between any two arbitrary functions f and g having continuous first and second derivative in the volume V bounded by the surface S :-

$$\iiint_V [gL(f) - fL(g)] dV = \iint_S (f \frac{\partial g}{\partial n} - g \frac{\partial f}{\partial n}) dS \quad (3.6)$$

where n is inward normal drawn to the surface S and L is Laplacian operator in cylindrical coordinates i.e. :-

$$L = \frac{\partial^2}{\partial \xi^2} + \frac{1}{\rho} \frac{\partial}{\partial \rho} + \frac{\partial^2}{\partial \rho^2} + \frac{1}{\rho^2} \frac{\partial^2}{\partial \nu^2}$$

here (ξ, ρ, ν) are running coordinates of domain V and S .

To obtain the solution for $\bar{\phi}$ one choses:

$$\begin{aligned} f(\xi, \rho, v) &= \bar{\phi}(\xi, \rho, v) \\ &= \bar{\phi}(\xi, \rho) \quad \text{because of axisymmetric} \\ &\quad \text{nature of } \phi \end{aligned}$$

$$\text{and } g(\xi, \rho, v) = \psi(\xi, \rho, v)$$

where ψ satisfies $L(\psi) = 0$ which gives the fundamental solution:

$$\psi = \frac{1}{4\pi R} \quad (3.7)$$

$$\text{where } R = [(\bar{x} - \xi)^2 + \bar{r}^2 + \rho^2 - 2\bar{r}\rho \cos(\theta - v)]^{1/2}$$

Then Equation (3.6) gives the integral equation :

$$\iiint_V \psi L(\bar{\phi}) dV = \iint_S (\bar{\phi} \frac{\partial \psi}{\partial n} - \psi \frac{\partial \bar{\phi}}{\partial n}) dS \quad (3.8)$$

Since ψ and $\bar{\phi}$ do not have continuous first and second derivatives everywhere in the flow field hence we shall investigate to what domain above relation holds. The volume is (unhatched portion in fig. 1) infinite volume V_T (enclosed by wall if wall is present) excluding (i) a spherical point cavity at $(\xi = \bar{x}, \rho = \bar{r}, v = \theta)$ where ψ is singular and (ii) the volume V_B which the body covers. The surface S bounding the volume V consists of

- i) surface S_T at ∞ for free air case or at wall if wall is present ;

- ii) surface S_P of spherical point cavity at
 $(\xi = \bar{x}, \rho = \bar{r}, \nu = \theta)$
 and iii) surface S_B bounded by the body.

Now we consider the volume and surface integral separately.

3.2.1 Volume Integral :

From equation (3.2)

$$\begin{aligned} L(\vec{\phi}) &= \vec{\phi}_{\xi} \vec{\phi}_{\xi\xi} \\ &= \frac{1}{2} \frac{\partial \bar{u}^2}{\partial \xi} \end{aligned}$$

where $\bar{u} = \vec{\phi}_{\xi}$

hence the volume integral in equation (3.8) becomes:

$$I_V = \frac{1}{2} \iiint_V \psi \frac{\partial \bar{u}^2}{\partial \xi} dV \quad (3.9)$$

here $V = V_T - V_P - V_B$

The cavity volume V_P can be included in V as it gives negligible contribution in the limit to (3.9) as shown below,

Let us assume the radius of spherical cavity to be ϵ , $\epsilon \rightarrow 0$, we get

$$dV = V_P = \frac{4}{3} \pi \epsilon^3$$

$$\frac{\partial \bar{u}^2}{\partial \xi} = \text{finite} = C_1(\text{say})$$

$$\begin{aligned} \therefore I_{V_P} &= \frac{1}{2} \iiint_{V_P} \psi \frac{\partial \bar{u}^2}{\partial \xi} dV \\ &= \frac{1}{2} \frac{1}{4\pi \epsilon} C_1 \frac{4}{3} \pi \epsilon^3 \\ &= \frac{1}{6} C_1 \epsilon^2 \\ &= 0 \quad \text{as } \epsilon \rightarrow 0 \end{aligned}$$

hence we get

$$V = V_T - V_B$$

Now integrating equation (3.9) by parts in ξ direction with boundary condition (3.4) of perturbation velocity vanishing at $\xi = \pm \infty$ one gets

$$I_V = - \frac{1}{2} \iiint_V \psi_{\xi} \bar{u}^2 dV \quad (3.10)$$

3.2.2 Surface Integral :

i) Integral over S_T :

For free air case the integral over the cylindrical surface S_{∞} at infinity can be expressed as

$$\begin{aligned} I_{S_T} &= I_{S_{\infty}} = \iint_{S_{\infty}} \left(\bar{\phi} \frac{\partial \psi}{\partial n} - \psi \frac{\partial \bar{\phi}}{\partial n} \right) dS \\ &= \lim_{\rho \rightarrow \infty} \int_{-\infty}^{\infty} \int_0^{2\pi} \left(\bar{\phi}_{\rho} \psi - \psi \bar{\phi}_{\rho} \right) \rho d\nu d\xi \end{aligned}$$

This integral, with ψ given by equation (3.7) and with the assumption that $\bar{\phi} \sim \frac{1}{(R)^c}$ for $c > 0$ at infinity, vanishes.

For wall interference case the integral over the finite cylindrical wall surface S_W can be expressed as

$$I_{S_T} = I_{S_W} = - \iint_{S_W} (\bar{\phi} \psi_\rho - \psi \bar{\phi}_\rho) \bar{r}_W dv d\xi$$

where \bar{r}_W is the radius of cylindrical wall

$$\text{or } I_{S_W} = \bar{r}_W \int_{-\infty}^{\infty} \int_0^{2\pi} (\psi \bar{\phi}_\rho - \bar{\phi} \psi_\rho)_{\rho=\bar{r}_W} dv d\xi$$

Applying porous wall boundary condition (3.5)

we get

$$I_{S_W} = - \bar{r}_W \int_{-\infty}^{\infty} \int_0^{2\pi} (\psi \frac{p}{\bar{p}} \bar{\phi}_\xi + \bar{\phi} \psi_\rho)_{\rho=\bar{r}_W} dv d\xi \quad (3.11)$$

After simplification equation (3.11) leads to following line integral (see Appendix A-I)

$$I_{S_W} = \int_{-\infty}^{\infty} [(A+B) \bar{\phi}(\xi, \bar{r}_W) - C \frac{p}{\bar{p}} \bar{\phi}_\xi(\xi, \bar{r}_W)] d\xi \quad (3.12)$$

where

$$A = \bar{r}_W \frac{\bar{r}_W - \bar{r}}{\pi} \frac{E(\pi/2, k)}{(a-b) \sqrt{a}}$$

$$B = \frac{1}{2\pi} \frac{F(\pi/2, k) - E(\pi/2, k)}{\sqrt{a}}$$

$$G = \frac{\bar{r}_w}{\pi} \frac{F(\pi/2, k)}{\sqrt{a}} \quad (3.13)$$

$$a = (\bar{x} - \xi)^2 + (\bar{r} + \bar{r}_w)^2; \quad b = 4 \bar{r} \bar{r}_w,$$

$$k = \sqrt{b/a}$$

E and F being the complete elliptic integral of second and first kind respectively.

Hence surface integral over S_T can be expressed as

$$I_{S_T} = \delta \int_{-\infty}^{\infty} \left[(A+B) \bar{\phi}(\xi, \bar{r}_w) - G \frac{p}{\beta} \bar{\phi}_{\xi}(\xi, \bar{r}_w) \right] d\xi \quad (3.14)$$

$$\text{where } \delta = \begin{cases} 0 & \text{for free air case} \\ 1 & \text{for wall interference case} \end{cases}$$

ii) Integral over S_P :

The point cavity is the sphere of radius ϵ , $\epsilon \rightarrow \infty$ around the point ($\xi = \bar{x}$, $\rho = \bar{r}$, $v = \theta$) the integral over S_P can be written as

$$\begin{aligned} I_{S_P} &= \iint_{S_P} \left(\bar{\phi} \frac{\partial \psi}{\partial n} - \psi \frac{\partial \bar{\phi}}{\partial n} \right) dS \\ &= \left[\bar{\phi}(\bar{x}, \bar{r}) \frac{\partial \psi}{\partial \bar{R}} - \psi \frac{\partial \bar{\phi}}{\partial \bar{R}} \right] 4\pi \epsilon^2 \\ &= \left[-\frac{\bar{\phi}(\bar{x}, \bar{r})}{4\pi \bar{R}^2} - \frac{1}{4\pi \bar{R}} \frac{\partial \bar{\phi}}{\partial \bar{R}} \right] 4\pi \epsilon^2 \\ &= -\bar{\phi}(\bar{x}, \bar{r}) - \epsilon \frac{\partial \bar{\phi}}{\partial \bar{R}} \quad (\text{since here } \bar{R} = \epsilon) \\ &= -\bar{\phi}(\bar{x}, \bar{r}) \quad \epsilon \rightarrow 0 \end{aligned} \quad (3.15)$$

iii) Integral over S_B :

$$I_{S_B} = \iint_{S_B} (\bar{\phi} \frac{\partial \psi}{\partial n} - \psi \frac{\partial \bar{\phi}}{\partial n}) dS$$

For sufficiently slender body we approximate:

$$\lim_{\rho \rightarrow 0} \frac{\partial}{\partial n} = \frac{\partial}{\partial \rho}$$

hence we get:

$$I_{S_B} = \int_0^l \int_0^{2\pi} (\bar{\phi} \frac{\partial \psi}{\partial \rho} - \psi \frac{\partial \bar{\phi}}{\partial \rho}) \rho d\nu d\xi \quad (3.16)$$

where l is the non dimensional length of the body.

In the limit $\rho \rightarrow 0$, $\bar{\phi}$ is of the form²⁷

$$\bar{\phi} = \frac{1}{2\pi} S'(\xi) \ln \rho + g(\xi) \quad (3.17)$$

Also from (3.7) :

$$\lim_{\rho \rightarrow 0} \psi_\rho = \frac{\bar{r} \cos(\theta - \nu)}{4\pi [(\bar{x} - \xi)^2 + \bar{r}^2]^{3/2}}$$

Hence in the limit as $\rho \rightarrow 0$, $\rho \bar{\phi} \psi_\rho = 0$ and the integral

(3.16) reduces to

$$I_{S_B} = - \lim_{\rho \rightarrow 0} \int_0^l \int_0^{2\pi} \psi \frac{\partial \bar{\phi}}{\partial \rho} \rho d\nu d\xi$$

Applying the tangency boundary condition (3.3):

$$I_{S_B} = - \lim_{\rho \rightarrow 0} \int_0^l \int_0^{2\pi} \frac{K}{\beta^2} \frac{S'(\xi)}{2\pi} \psi d\nu d\xi$$

$$= -\frac{K}{4\pi\beta^2} \int_0^{\ell} \frac{S'(\xi)}{\sqrt{(\bar{x}-\xi)^2 + \bar{r}^2}} d\xi \quad (3.18)$$

Now using (3.10), (3.14), (3.15) and (3.18) in Green's Theorem (3.8) we finally obtain, a non-linear integral equation for $\bar{\phi}$

$$\begin{aligned} \bar{\phi}(\bar{x}, \bar{r}) = & -\frac{K}{4\pi\beta^2} \int_0^{\ell} \frac{S'(\xi)}{\sqrt{(\bar{x}-\xi)^2 + \bar{r}^2}} d\xi \\ & + \delta \int_{-\infty}^{\infty} [A+B] \bar{\phi}(\xi, \bar{r}_w) - \frac{p}{\beta} \bar{\phi}_{\xi}(\xi, \bar{r}_w) d\xi \\ & + \frac{1}{2} \iiint_V \psi_{\xi} \bar{\phi}_{\xi}^2(\xi, \rho) dV \end{aligned} \quad (3.19)$$

Now to obtain an equation for the axial perturbation velocity we differentiate equation (3.20) w.r.t. \bar{x} (see Appendix A-II) and we get :

$$\begin{aligned} \bar{u}(\bar{x}, \bar{r}) = & \frac{K}{4\pi\beta^2} \int_0^{\ell} \frac{S'(\xi)(\bar{x}-\xi)}{[(\bar{x}-\xi)^2 + \bar{r}^2]^{3/2}} d\xi \\ & + \delta \int_{-\infty}^{\infty} [A+B+D] \bar{u}(\xi, \bar{r}_w) d\xi \\ & + \frac{1}{2} \iiint_V \psi_{\xi\bar{x}} \bar{u}^2 dV \end{aligned} \quad (3.20)$$

where $D = \frac{p}{\beta} \frac{\bar{x}-\xi}{\bar{r}_w - \bar{r}} A$

and A, B stand for same notations as defined in (3.13).

The equation (3.20) can be rewritten as

$$\begin{aligned} \bar{u}(\bar{x}, \bar{r}) = & \bar{u}_L(\bar{x}, \bar{r}) + \delta \int_{-\infty}^{\infty} (A+B+D) \bar{u}(\xi, \bar{r}_w) d\xi \\ & + \frac{1}{2} \iiint_V \psi_{\xi} \bar{x} \bar{u}^2(\xi, \rho) dV \end{aligned} \quad (3.21)$$

where $\bar{u}_L(\bar{x}, \bar{r}) = \frac{K}{\beta^2} u_L(\bar{x}, \bar{r})$

$$u_L = \frac{1}{4\pi} \int_0^{\ell} \frac{S'(\xi) (\bar{x} - \xi)}{[(\bar{x} - \xi)^2 + \bar{r}^2]^{3/2}} d\xi$$

u_L being the linear value of perturbation velocity.

3.3 Two- Dimensional Flow

In previous section we derived axial velocity perturbation for axisymmetric flow. In the same manner the axial velocity perturbation in two dimensional flow over thin airfoil at zero incidence has been derived in this section.

We first introduce the similar transformation i.e.

$$\bar{x} = x ; \quad \bar{y} = \beta y ; \quad \bar{\phi} = \frac{K}{\beta^2} \phi \quad (3.22)$$

where $\beta = \sqrt{1 - M_{\infty}^2}$ and $K = (\gamma + 1) M_{\infty}^2$

Using (3.22) in the governing transonic flow equation (2.8) and boundary conditions (2.9), (2.10) and (2.11), we obtain

$$\bar{\phi}_{\bar{x}\bar{x}} + \bar{\phi}_{\bar{y}\bar{y}} = \bar{\phi}_{\bar{x}} \bar{\phi}_{\bar{x}\bar{x}} \quad (3.23)$$

$$\bar{\phi}_{\bar{y}}(\bar{x}, 0^{\pm}) = \frac{d\bar{Y}_{\pm}(\bar{x})}{d\bar{x}} \quad (3.24)$$

where $\bar{Y}_{\pm}(\bar{x}) = \frac{K}{\beta^2} Y_{\pm}(x)$

$$\bar{\phi}_{\bar{x}}, \bar{\phi}_{\bar{y}} \rightarrow 0 \quad \text{at infinity} \quad (3.25)$$

and for the wall interference case, at the wall $\bar{y} = \pm \bar{y}_w$

$$\bar{\phi}_{\bar{y}} = \mp \frac{p}{\beta} \bar{\phi}_{\bar{x}} \quad (3.26)$$

For two-dimensional case the Green's Theorem which relates the surface integral to line integral is :

$$\iint_S [gL(f) - fL(g)] dS = \int_G (f \frac{\partial g}{\partial n} - g \frac{\partial f}{\partial n}) dC \quad (3.27)$$

where f and g are arbitrary function having continuous first and second derivative in surface $S = S(\xi, \zeta)$ bounded by curve $G = G(\xi, \zeta)$ and n is the inward drawn normal to the boundary. L is the Laplacian operator given by

$$L = \frac{\partial^2}{\partial \xi^2} + \frac{\partial^2}{\partial \zeta^2}$$

To investigate the solution for $\bar{\phi}$, we choose:

$$f = \bar{\phi}(\xi, \zeta)$$

and $g = \psi$

where ψ satisfies the Laplace equation $L(\psi) = 0$. The fundamental solution of this equation is :

$$\psi = \ln \bar{R} \quad (3.28)$$

$$\text{where } \bar{R} = \sqrt{(\xi - \bar{x})^2 + (\zeta - \bar{y})^2}$$

Hence equation (3.27) together with equation (3.23) gives us:

$$\iint_S \psi \bar{\zeta} \bar{\zeta}_{\xi\xi} dS = \int_G (\bar{\zeta} \frac{\partial \psi}{\partial n} - \psi \frac{\partial \bar{\zeta}}{\partial n}) dG \quad (3.29)$$

Now we shall investigate the surface S and bounding curve G where ψ and $\bar{\zeta}$ have continuous first and second derivative keeping in view the boundary condition.

Such surface is infinite plane S_T (enclosed by wall if wall is present) excluding (i) a circular point cavity S_P at $(\xi = \bar{x}, \zeta = \bar{y})$ and (ii) the airfoil surface S_B . (see fig. 2).

The curve G consists of (i) curve G_T around infinite plane (or wall if wall is present) (ii) Curve G_P around circular cavity and (iii) curve G_B around airfoil surface. (see fig. 2).

Now we shall analyse the surface and line integrals of equation (3.29).

3.3.1 Surface Integral:

From equation (3.29) integral over surface is given by

$$\begin{aligned} I_S &= \iint_S \psi \bar{\phi}_\xi \bar{\phi}_{\xi t} dS \\ &= \frac{1}{2} \iint_S \psi \frac{\partial}{\partial \xi} \bar{u}^2 dS \end{aligned} \quad (3.30)$$

here $S = S_T - S_P - S_B$

The cavity surface S_P can be included in S as it gives zero contribution in the limit to (3.30) as shown below.

Let radius of circular cavity be ϵ , $\epsilon \rightarrow 0$, we get:

$$\begin{aligned} dS &= 4\pi \epsilon^2 \\ \frac{\partial}{\partial \xi} \bar{u}^2 &= \text{finite} = C_2 (\text{say}) \\ \therefore I_{S_P} &= \frac{1}{2} (\ln \epsilon) C_2 4\pi \epsilon^2 \quad (\text{since here } \bar{R} = \epsilon) \\ &= 0 \quad \text{as } \epsilon \rightarrow 0. \end{aligned}$$

hence we get:

$$S = S_T - S_B$$

Now integrating equation (3.30) by parts in ξ direction with the boundary condition of perturbation velocity vanishing at infinity we get :

$$I_S = - \frac{1}{2} \iint_S \psi_\xi \bar{u}^2 dS \quad (3.31)$$

3.3.2 Line integral :

i) Integral over C_T :

Since all perturbation vanish at infinity hence for free air case integral over C_T gives zero contribution while for wall interference case integral over C_T gives a finite value I_{C_T} given by (see Appendix B)

$$I_{C_T} = -\delta \int_{-\infty}^{\infty} \bar{\phi}_{\xi}(\xi, \bar{y}_w) \left\{ \frac{p}{\rho} [\psi(\zeta = \bar{y}_w) + \psi(\zeta = -\bar{y}_w)] - \int [\psi_{\zeta}(\zeta = \bar{y}_w) - \psi_{\zeta}(\zeta = -\bar{y}_w)] d\xi \right\} d\xi \quad (3.3.2)$$

where $\delta = \begin{cases} 0 & \text{for free air} \\ 1 & \text{for wall interference case} \end{cases}$

and $\zeta = \begin{cases} \bar{y}_w & \text{at upper wall} \\ -\bar{y}_w & \text{at lower wall} \end{cases}$

ii) Integral over C_P :

Integral over curve C_P is given as follows

$$\begin{aligned} I_{C_P} &= \int_{C_P} (\bar{\phi} \psi_n - \psi \bar{\phi}_n) dC \\ &= [\bar{\phi}(\bar{x}, \bar{y}) \frac{\partial \psi}{\partial R} - \psi \frac{\partial \bar{\phi}}{\partial R}] 2\pi\epsilon \end{aligned}$$

where $\epsilon, \epsilon \rightarrow 0$ is radius of circular cavity C_P .

again $I_{C_P} = 2\pi \bar{\phi}(\bar{x}, \bar{y}) - 2\pi \epsilon \ln \epsilon \frac{\partial \bar{\phi}}{\partial \bar{R}}$

(since here $\bar{R} = \epsilon$)

$$= 2\pi \bar{\phi}(\bar{x}, \bar{y}) \quad \text{as } \epsilon \rightarrow 0 \quad (3.33)$$

iii) Integral over C_B :

Integral over body curve C_B is given by :

$$\begin{aligned} I_{C_B} &= \int_{C_B} (\bar{\phi} \psi_n - \psi \phi_n) dC \\ &= - \int_0^1 \left[\ln [(\bar{x} - \xi)^2 + (\bar{y} - \zeta)^2]^{1/2} \Delta \bar{\phi}_\zeta \right. \\ &\quad \left. - \Delta \bar{\phi} \frac{\zeta - \bar{y}}{(\xi - \bar{x})^2 + (\zeta - \bar{y})^2} \right]_{\zeta=0} d\xi \end{aligned}$$

here $\Delta \bar{\phi}_\zeta = \bar{\phi}_\zeta(\bar{x}, 0^+) - \bar{\phi}_\zeta(\bar{x}, 0^-)$

$$\Delta \bar{\phi} = \bar{\phi}(\bar{x}, 0^+) - \bar{\phi}(\bar{x}, 0^-)$$

$$= 0 \quad \text{for symmetric airfoil at zero incidence}$$

from boundary condition (3.24) we get:

$$\begin{aligned} \Delta \bar{\phi}_\zeta &= \frac{d\bar{Y}_+(\xi)}{d\xi} - \frac{d\bar{Y}_-(\xi)}{d\xi} \\ &= 2 \frac{d\bar{Y}_+}{d\xi} \quad \text{for symmetric airfoil at zero incidence.} \end{aligned}$$

which leads to

$$I_{C_B} = -2 \int_0^1 \ln [(\xi - \bar{x})^2 + \bar{y}^2]^{1/2} \frac{d\bar{Y}_+(\xi)}{d\xi} d\xi \quad (3.34)$$

Combining (3.31), (3.32), (3.33) and (3.34) in equation (3.29) we get integral equation for the transformed velocity potential as

$$\begin{aligned}\bar{\phi}(\bar{x}, \bar{y}) = & \frac{1}{\pi} \int_0^1 \ln [(\xi - \bar{x})^2 + \bar{y}^2]^{1/2} \frac{d\bar{Y}_+(\xi)}{d\xi} d\xi \\ & + \frac{\delta}{2\pi} \int_{-\infty}^{\infty} \bar{\phi}_{\xi}(\xi, \bar{y}_w) \left\{ \frac{p}{\beta} [\psi(\zeta = \bar{y}_w) + \psi(\zeta = -\bar{y}_w)] \right. \\ & \left. - \int [\psi_{\zeta}(\zeta = \bar{y}_w) - \psi_{\zeta}(\zeta = -\bar{y}_w)] d\xi \right\} d\xi \\ & - \frac{1}{4\pi} \iint \psi_{\xi} \bar{\phi}_{\xi}^2 d\xi d\zeta\end{aligned}\quad (3.35)$$

To obtain integral equation for axial component of perturbation velocity we differentiate equation (3.35) w.r.t. \bar{x} .

Thus

$$\begin{aligned}\bar{u}(\bar{x}, \bar{y}) = & \frac{K}{\pi\beta^3} \int_0^1 \frac{\bar{x} - \xi}{[(\bar{x} - \xi)^2 + \bar{y}^2]} \frac{dY_+(\xi)}{d\xi} d\xi \\ & - \frac{\delta}{2\pi} \int_{-\infty}^{\infty} \bar{\phi}_{\xi}(\xi, \bar{y}_w) \left\{ \frac{p}{\beta} [\psi_{\xi}(\zeta = \bar{y}_w) \right. \\ & \left. + \psi_{\xi}(\zeta = -\bar{y}_w)] - \psi_{\zeta}(\zeta = \bar{y}_w) + \psi_{\zeta}(\zeta = -\bar{y}_w) \right\} d\xi \\ & - \frac{1}{4\pi} \iint_S \psi_{\xi} \bar{x} \bar{u}^2 d\xi d\zeta \\ \text{or } \bar{u}(\bar{x}, \bar{y}) = & \bar{u}_L(\bar{x}, \bar{y}) - \frac{\delta}{2\pi} \int_{-\infty}^{\infty} \bar{u}(\xi, \bar{y}_w) \left\{ \frac{p}{\beta} [\psi_{\xi}(\zeta = \bar{y}_w) \right. \\ & \left. + \psi_{\xi}(\zeta = -\bar{y}_w)] - \psi_{\zeta}(\zeta = \bar{y}_w) + \psi_{\zeta}(\zeta = -\bar{y}_w) \right\} d\xi \\ & - \frac{1}{4\pi} \iint_S \psi_{\xi} \bar{x} \bar{u}^2 d\xi d\zeta\end{aligned}\quad (3.36)$$

where $\bar{u}_L(\bar{x}, \bar{y}) = \frac{K}{\beta^2} u_L(\bar{x}, \bar{y})$

$$\text{and } u_L(\bar{x}, \bar{y}) = \frac{1}{\pi\beta} \int_0^1 \frac{\bar{x} - \xi}{[(\bar{x} - \xi)^2 + \bar{y}^2]} \frac{dY_+(\xi)}{d\xi} d\xi \quad (3.37)$$

here u_L is linear value of perturbation velocity for symmetric airfoil at zero incidence.

CHAPTER 4

NUMERICAL SCHEME

4.1 Introduction:

In this chapter a numerical scheme is presented which has been used in calculating integrals involved in computation of perturbation velocity. The integrals have been suitably expressed in summation form approximating velocity perturbation to be constant in small intervals. In this manner a set of algebraic equations are formed which are solved by method of iteration using suitable convergence criteria.

4.2 Axisymmetric Flow :

We consider equation (3.21) for numerical evaluation. $u_L(\bar{x}, \bar{r})$ for general axisymmetric body can be calculated numerically as follows.

$$u_L(\bar{x}, \bar{r}) = \frac{1}{4\pi} \int_0^l \frac{S'(\xi)(\bar{x}-\xi)}{[(\bar{x}-\xi)^2 + \bar{r}^2]^{3/2}} d\xi$$

which on integration by parts give

$$u_L(\bar{x}, \bar{r}) = \frac{1}{4\pi} \left[\frac{S'(l)}{\sqrt{(l-\bar{x})^2 + \bar{r}^2}} + S''(\bar{x}) \ln \frac{\bar{r}^2}{4\bar{x}(l-\bar{x})} + \int_0^l \frac{S''(\bar{x}) - S''(\xi)}{\sqrt{(\bar{x}-\xi)^2 + \bar{r}^2}} d\xi \right] \quad (4.1)$$

I.I.T. KANPUR
CENTRAL LIBRARY
No. A-62204

On the body surface $r = R(x)$ or $\bar{r} = \beta R$ equation (4.1) for pointed nosed bodies simplifies to

$$u_L(\bar{x}, 0) = \frac{1}{4\pi} \left[\frac{S'(\ell)}{|\ell - \bar{x}|} + S''(\bar{x}) \ln \frac{\beta^2 R^2}{4\bar{x}(\ell - \bar{x})} + \int_0^\ell \frac{S''(\bar{x}) - S''(\xi)}{|\bar{x} - \xi|} d\xi \right] \quad (4.2)$$

The integral in eq. (4.2) vanishes for $\xi = \bar{x}$. The Simpson's rule can be used to evaluate this integral quite satisfactorily.

For the evaluation of linear perturbation velocity away from the body, following procedure has been adopted:

$$\begin{aligned} u_L(\bar{x}, \bar{r}) &= \frac{1}{4\pi} \sum_{i=1}^{n_1} S'(\bar{x}_i) \int_{\bar{x}_i - l_i}^{\bar{x}_i + l_i} \frac{\bar{x} - \xi}{[(\bar{x} - \xi)^2 + \bar{r}^2]^{3/2}} d\xi \\ &= \frac{1}{4\pi} \sum_{i=1}^{n_1} S'(\bar{x}_i) \left[\frac{1}{(\bar{x} - \bar{x}_i - l_i)^{1/2}} - \frac{1}{(\bar{x} - \bar{x}_i + l_i)^{1/2}} \right] \end{aligned} \quad (4.3)$$

where $x_1 = l_1 = 0$

and $x_{n_1} = l_{n_1} = \ell$

Here the body length has been divided into n_1 numbers of intervals of width $2l_i$.

Before considering equation (3.22) we attach a subscript S to \bar{x} and P to \bar{r} to simplify the analysis further. The second expression on RHS of equation (3.21) can then be expressed as :

$$\begin{aligned} & \delta \int_{-\infty}^{\infty} (A + B + D) \bar{u}(\xi, \bar{r}_w) d\xi \\ &= \delta \sum_{i=1}^n b_{iwSP} \bar{u}_{iw} \end{aligned} \quad (4.4)$$

where $\bar{u}_{iw} = \bar{u}(\bar{x}_i, \bar{r}_w)$

$$\text{and } b_{iwSP} = \int_{\bar{x}_i - \delta_i}^{\bar{x}_i + \delta_i} (A + B + D) d\xi$$

Here the wall has been divided into n number of steps of size $2\delta_i$ and the velocity at the mid point of each step has been assumed constant over that step.

To simplify b_{iwSP} further we proceed as in Appendix C and finally obtain :

$$\begin{aligned} b_{iwSP} = & \frac{E[\pi/2, k(X_3^w)]}{2\pi} \sqrt{\frac{\bar{r}_w}{\bar{r}_P}} \left[\tan^{-1} \frac{X_1}{(\bar{r}_w - \bar{r}_P)} k(X_1^w) \right. \\ & - \tan^{-1} \frac{X_2}{(\bar{r}_w - \bar{r}_P)} k(X_2^w) - \frac{p}{2\beta} \ln \frac{1-k(X_2^w)}{1+k(X_2^w)} \frac{1+k(X_1^w)}{1-k(X_1^w)} \Big] \\ & + \frac{E[\pi/2, k(X_3^w)] - E[\pi/2, k(X_3^w)]}{2\pi} \\ & \ln \frac{\sqrt{X_2^2 + (\bar{r}_w + \bar{r}_P)^2} - X_2}{\sqrt{X_1^2 + (\bar{r}_w + \bar{r}_P)^2} - X_1} \end{aligned} \quad (4.5)$$

$$\begin{aligned}
\text{where } X_1 &= \bar{x}_S - \bar{x}_i + \delta_i \\
X_2 &= \bar{x}_S - \bar{x}_i - \delta_i \\
X_3 &= \bar{x}_S - \bar{x}_i \\
k(X^w) &= \sqrt{\frac{4 \bar{r}_P \bar{r}_W}{X^2 + (\bar{r}_W + \bar{r}_P)^2}}
\end{aligned}$$

To evaluate the volume integral of equation (3.21) the region of integration has been divided in rectangular grid in meridian plane. The computational domain is defined by grid network as shown in fig. 3. The perturbation velocity at the centre of a grid has been taken constant throughout that grid. Hence we get the volume integral after simplification as (see Appendix D)

$$\begin{aligned}
& \frac{1}{2} \iiint_V \psi_{\xi \bar{x}} \bar{u}^2 (\xi, \rho) dV \\
&= \sum_{i=1}^n \sum_{j=1}^m \bar{u}_{ij}^2 a_{ijSP}
\end{aligned} \tag{4.6}$$

where $\bar{u}_{ij} = \bar{u}(\bar{x}_i, \bar{r}_j)$

$$\begin{aligned}
\text{and } a_{ijSP} &= \frac{1}{2} \int_{\bar{r}_j - q_j}^{\bar{r}_j + h_j} \int_0^{2\pi} \int_{\bar{x}_i - \delta_i}^{\bar{x}_i + \delta_i} \psi_{\xi \bar{x}} \rho d\xi dv d\rho \\
&= \frac{1}{2\pi} [G(X_1) E(\pi/2, k(X_1)) T(X_1) \\
&\quad - G(X_2) E(\pi/2, k(X_2)) T(X_2)]
\end{aligned} \tag{4.7}$$

$$\text{where } G(X) = \frac{\bar{r}_j}{\sqrt{X^2 + (\bar{r}_P + \bar{r}_j)^2}}$$

$$T(X) = \tan^{-1} \frac{\bar{r}_j - \bar{r}_P + h_j}{X} - \tan^{-1} \frac{\bar{r}_j - \bar{r}_P - q_j}{X}$$

$$k(X) = \sqrt{\frac{4 \bar{r}_P \bar{r}_j}{X^2 + (\bar{r}_P + \bar{r}_j)^2}}$$

Finally using (4.4) and (4.6), equation (3.21) can be expressed in iterative form as

$$\bar{u}_{SP}^{(n)} = \bar{u}_{LSP} + \delta \sum_{i=1}^n b_{iWSP} \bar{u}_{iW}^{(n-1)} + \sum_{i=1}^n \sum_{j=1}^m a_{ijSP} \bar{u}_{ij}^{2(n-1)} \quad (4.8)$$

$$= g \text{ (say)}$$

$$\text{where } \bar{u}_{SP} = \bar{u}(\bar{x}_S, \bar{r}_P)$$

$$\text{and } \bar{u}_{LSP} = \bar{u}_L(\bar{x}_S, \bar{r}_P)$$

For convergence of above iterative equation $\lambda \bar{u}_{SP}$ has been added to both sides where $\lambda = -\frac{\partial g}{\partial \bar{u}_{SP}} = -2 a_{SPSP} \bar{u}_{SP}$, so that we obtain

$$\begin{aligned} \bar{u}_{SP}^{(n)} = & \left[\bar{u}_{LSP} + \delta \sum_{i=1}^n b_{iWSP} \bar{u}_{iW}^{(n-1)} + \sum_{i=1}^n \sum_{j=1}^m a_{ijSP} \bar{u}_{ij}^{2(n-1)} \right. \\ & \left. - 2 a_{SPSP} \bar{u}_{SP}^{(n-1)} \right] / \left[1 - 2 a_{SPSP} \bar{u}_{SP}^{(n-1)} \right] \quad (4.9) \end{aligned}$$

The convergence is achieved provided $a_{SPSP} \neq 0.5/\bar{u}_{SP}$

4.3 Two-dimensional Flow :

The numerical iterative form of the integral equation (3.36) for two-dimensional case can be obtained in the similar way as in § 4.2.

For most of the two-dimensional airfoils analytical results are available for linear value of velocity potential. These results for parabolic airfoils and NACA OOX airfoils are presented in Appendix E-II .

The wall integral in equation (3.37) is numerically expressed as

$$\begin{aligned}
 & - \frac{\delta}{2\pi} \int_{-\infty}^{\infty} \bar{u}(\xi, \bar{y}_w) \left\{ \frac{p}{\beta} [\psi_{\xi}(\zeta = \bar{y}_w) + \psi_{\xi}(\zeta = -\bar{y}_w)] \right. \\
 & \quad \left. - \psi_{\zeta}(\zeta = \bar{y}_w) + \psi_{\zeta}(\zeta = -\bar{y}_w) \right\} d\xi \\
 & = \delta \sum_{i=1}^n d_{iWSP} \bar{u}_{iW}
 \end{aligned}$$

where $\bar{u}_{iW} = \bar{u}(\bar{x}_i, \bar{y}_w)$

introducing $\bar{x} = \bar{x}_S$ and $\bar{y} = \bar{y}_P$

$$\begin{aligned}
 d_{iWSP} & = - \frac{1}{2\pi} \int_{\bar{x}_i - \delta_i}^{\bar{x}_i + \delta_i} \left\{ \frac{p}{\beta} [\psi_{\xi}(\zeta = \bar{y}_w) + \psi_{\xi}(\zeta = -\bar{y}_w)] \right. \\
 & \quad \left. - \psi_{\zeta}(\zeta = \bar{y}_w) + \psi_{\zeta}(\zeta = -\bar{y}_w) \right\} d\xi
 \end{aligned}$$

$$\begin{aligned}
&= - \frac{1}{2\pi} \left\{ \frac{p}{\beta} \left[\psi(\zeta = \bar{y}_w) + \psi(\zeta = -\bar{y}_w) \right] \frac{\bar{x}_i + \delta_i}{\bar{x}_i - \delta_i} \right. \\
&\quad \left. + \left[\tan^{-1} \frac{\bar{x}_S - \xi}{\bar{y}_w - \bar{y}_P} + \tan^{-1} \frac{\bar{x}_S - \xi}{\bar{y}_w + \bar{y}_P} \right] \frac{\bar{x}_i + \delta_i}{\bar{x}_i - \delta_i} \right\} \\
&= - \frac{1}{2\pi} \left\{ \frac{p}{2\beta} \left[\ln \frac{(\bar{y}_w - \bar{y}_P)^2 + x_2^2}{(\bar{y}_w - \bar{y}_P)^2 + x_1^2} \cdot \frac{(\bar{y}_w + \bar{y}_P)^2 + x_2^2}{(\bar{y}_w + \bar{y}_P)^2 + x_1^2} \right] \right. \\
&\quad + \tan^{-1} \frac{x_2}{\bar{y}_w - \bar{y}_P} - \tan^{-1} \frac{x_1}{\bar{y}_w - \bar{y}_P} + \tan^{-1} \frac{x_2}{\bar{y}_w + \bar{y}_P} \\
&\quad \left. - \tan^{-1} \frac{x_1}{\bar{y}_w + \bar{y}_P} \right\}
\end{aligned}$$

where $x_1 = \bar{x}_S - \bar{x}_i + \delta_i$

$$x_2 = \bar{x}_S - \bar{x}_i - \delta_i$$

Before representing surface integral of equation (3.36) in suitable form for numerical evaluation we use the symmetric property of $\bar{u}(\xi, \zeta)$ for symmetric flow and limit the integration region to upper half plane only, as follows:

$$\begin{aligned}
&= \frac{1}{4\pi} \iint_S \psi_{\xi \bar{x}} \bar{u}^2 d\xi d\zeta \\
&= - \frac{1}{4\pi} \int_{-\infty}^{\infty} \int_{-\bar{y}_T}^{\bar{y}_T} \frac{(\xi - \bar{x}_S)^2 - (\zeta - \bar{y}_P)^2}{[(\xi - \bar{x}_S)^2 + (\zeta - \bar{y}_P)^2]^2} \bar{u}^2(\xi, \zeta) d\zeta d\xi \\
&\quad (\bar{y}_T \text{ is extent of } \zeta) \\
&= - \frac{1}{4\pi} \int_{-\infty}^{\infty} \int_0^{\bar{y}_T} \left[\frac{(\xi - \bar{x}_S)^2 - (\zeta - \bar{y}_P)^2}{[(\xi - \bar{x}_S)^2 + (\zeta - \bar{y}_P)^2]^2} + \right. \\
&\quad \left. + \frac{(\xi - \bar{x}_S)^2 - (\zeta + \bar{y}_P)^2}{[(\xi - \bar{x}_S)^2 + (\zeta + \bar{y}_P)^2]^2} \right] \bar{u}(\xi, \zeta) d\zeta d\xi
\end{aligned}$$

$$= Z \text{ (say)}$$

Now the region of integration is divided into rectangular elements, as shown in Fig. 4. The perturbation velocity at the centre of each element is assumed constant within that element. This gives :

$$Z = \sum_{i=1}^n \sum_{j=1}^m a_{ijSP} \bar{u}_{ij}^2$$

$$\text{where } \bar{u}_{ij} = \bar{u}(\bar{x}_i, \bar{y}_j)$$

$$\begin{aligned} a_{ijSP} &= - \frac{1}{4\pi} \int_{\bar{y}_j - q_j}^{\bar{y}_j + h_j} \int_{\bar{x}_i - \delta_i}^{\bar{x}_i + \delta_i} \left[\frac{(\xi - \bar{x}_S)^2 - (\zeta - \bar{y}_P)^2}{[(\xi - \bar{x}_S)^2 + (\zeta - \bar{y}_P)^2]^2} \right. \\ &\quad \left. + \frac{(\xi - \bar{x}_S)^2 - (\zeta + \bar{y}_P)^2}{[(\xi - \bar{x}_S)^2 + (\zeta + \bar{y}_P)^2]^2} \right] d\xi d\zeta \\ &= - \frac{1}{4\pi} \int_{\bar{y}_j - q_j}^{\bar{y}_j + h_j} \left[\frac{\bar{x}_S - \xi}{(\xi - \bar{x}_S)^2 + (\zeta - \bar{y}_P)^2} + \frac{\bar{x}_S - \xi}{(\xi - \bar{x}_S)^2 + (\zeta + \bar{y}_P)^2} \right] d\zeta \\ &= - \frac{1}{4\pi} \int_{\bar{y}_j - q_j}^{\bar{y}_j + h_j} \left[\frac{x_2}{x_2^2 + (\zeta - \bar{y}_P)^2} + \frac{x_2}{x_2^2 + (\zeta + \bar{y}_P)^2} \right. \\ &\quad \left. - \frac{x_1}{x_1^2 + (\zeta - \bar{y}_P)^2} - \frac{x_1}{x_1^2 + (\zeta + \bar{y}_P)^2} \right] d\zeta \\ &= - \frac{1}{4\pi} \left[\tan^{-1} \frac{\bar{y}_P + \zeta}{x_2} - \tan^{-1} \frac{\bar{y}_P - \zeta}{x_2} - \tan^{-1} \frac{\bar{y}_P + \zeta}{x_1} \right. \\ &\quad \left. + \tan^{-1} \frac{\bar{y}_P - \zeta}{x_1} \right] \Big|_{\bar{y}_j - q_j}^{\bar{y}_j + h_j} \end{aligned}$$

$$= - \frac{1}{4\pi} \left[\tan^{-1} \frac{Y_4}{X_2} - \tan^{-1} \frac{Y_3}{X_2} - \tan^{-1} \frac{Y_2}{X_2} + \tan^{-1} \frac{Y_1}{X_2} \right. \\ \left. - \tan^{-1} \frac{Y_4}{X_1} + \tan^{-1} \frac{Y_3}{X_1} + \tan^{-1} \frac{Y_2}{X_1} - \tan^{-1} \frac{Y_1}{X_1} \right]$$

$$Y_1 = \bar{y}_P - \bar{y}_j + q_j ; \quad Y_3 = \bar{y}_P + \bar{y}_j - q_j$$

$$Y_2 = \bar{y}_P - \bar{y}_j - h_j ; \quad Y_4 = \bar{y}_P + \bar{y}_j + h_j$$

Thus equation (3.36) in iterative form becomes

$$\bar{u}_{SP}^{(n)} = \bar{u}_{SP}^{(n-1)} + \delta \sum_{i=1}^n d_{iwSP} \bar{u}_{iw}^{(n-1)} + \sum_{i=1}^n \sum_{j=1}^m a_{ijSP} \bar{u}_{ij}^{(n-1)} \quad (4.10)$$

where $\bar{u}_{SP} = \bar{u}(\bar{x}_S, \bar{y}_P)$

and $\bar{u}_{LSP} = \bar{u}_L(\bar{x}_S, \bar{y}_P)$

CHAPTER 5

RESULTS AND DISCUSSION

5.1 Introduction:-

In this chapter results of computations are presented and discussed. Results are computed at zero angle of attack for parabolic arc of revolution, parabolic airfoil and NACA-0012 airfoil. They are compared with experimental results and/or that obtained by relaxation technique. The discussion for axisymmetric flow and two dimensional flow are dealt with separately. Listing of the computer programmes is given in Appendix F. The computations were carried out on DEC-1090 System.

5.2 Axisymmetric Flow :-

Various results for parabolic arc of revolution of fineness ratio 10 with sting at 0.854 have been obtained at different Mach numbers in free air and in the presence of wind tunnel wall. The aft and fore effects are also included.

For free air case integration was carried out in the range $0.28 \leq x \leq 1.16$ and $0 \leq r \leq 1.1$. The streamwise grid size of $\Delta x = .04$ was chosen. The transverse grid size Δr in physical plane was .2 except on the body surface where it was .1. Overall 37×6 rectangular elements were taken.

Fig. 5 shows distribution of C_p on the body at Mach number 0.9. It agrees quite satisfactorily with Bailey²⁰ and

experimental results of Taylor and McDevitt²⁹ except in mid region. The results for this case are also presented away from the body and compared with experimental results²⁹ (see fig. 6). The convergence is achieved in 4 iterations.

Fig. 7 shows a comparison between present result with porous wall at radius 1.17 and porosity parameter 0.77, with the experimental result²⁹ carried out in similar conditions²⁰. They are in close agreement except near the sting. The integration was carried out in the range $0 \leq x \leq 0.854$ and $0 \leq r \leq 1.17$ without taking fore and aft effects at Mach number 0.9. It took 14 iterations to converge which indicates the porous wall interaction with flow perturbations. The results are plotted on and away from the body.

Fig. 8 shows a comparison between three cases i) body in free air ii) body in presence of porous wall with porosity parameter 0.77 and iii) body in presence of solid wall, at Mach number 0.85. The axial integration range was $-.28 \leq x \leq 1.16$ and the wall was taken at radius 1.17. For convergence the number of iterations were 3, 9 and 5 respectively. The porous wall case do not have much difference over free air case. In the solid wall case the flow shows increased acceleration in the mid region.

A comparison between free air case and solid wall case at Mach no. 0.9 with fore and aft effects is shown in fig. 9.

More increased acceleration of the flow is observed here in mid region which signifies that with increase of Mach number the effect of wall interference increases. The convergence was achieved in 4 and 10 iterations respectively for the two cases. Porous wall interference calculations did not converge in the limit of 15 iterations. However, without for and aft effects it converged in 14 iterations as mentioned above. Correspondingly solid wall and free air calculations were done without fore and aft effects (see fig. 10). They took 8 and 4 iterations respectively.

The present method works also for shock-free supercritical case at Mach numbers 0.950 and 0.955 for free air with aft and fore body effects. Convergence was achieved in 7 and 10 iterations respectively. The pressure distribution on body surface is presented in fig. 11. The result of Mach number 0.950 shows agreeable matching with experimental results²⁹.

Fig. 12 shows a sample calculation for general parabolic body of revolution having maximum thickness at 30 percent and 70 percent of body length. Convergence was achieved in 4 and 5 iterations respectively at Mach numbers 0.9 with aft and fore effects.

The CPU time varies from 40 secs to 1.2 minutes depending on number of iterations taken.

5.3 Two-Dimensional Flow

The computations were carried out for NACA-0012 airfoil and 6 percent thick parabolic arc airfoil.

Pressure coefficient over NACA-0012 airfoil was obtained at Mach number 0.72 in free air. The integration was carried out in the range $-.28 \leq x \leq 1.28$ and $-.9.12 \leq y \leq 9.12$ and 39×6 rectangular elements were chosen with streamwise grid size $\Delta x = .04$ convergence was achieved in 6 iterations taking 2 minutes of CPU time. The results were compared with Lock's³¹ finite difference numerical results. They match well near the peak, however, present is slightly lower negative at other points (see fig. 13).

Results of 6 percent thick airfoil is given in fig. 14, 15 and 16. The integration was carried out in the range $0 \leq x \leq 1$ and $-4.56 \leq y \leq 4.56$. 25×6 rectangular elements were chosen with streamwise grid size $\Delta x = .04$. Fig 14 shows a comparison between the result obtained by Steger¹⁹ and present method at Mach no. .825. Result for present method was found slightly lower negative than that of Steger's. Convergence was achieved in 5 iterations taking 40 secs of CPU time. Fig. 15 shows the effect of solid wall on the pressure coefficient on the body at Mach number .825. The wall was taken at $(h/C) = 2.0$ and range of integration was $0 \leq x \leq 1$ and $-2 \leq y \leq 2$ with 25×6 grid points. The

solid wall interference gives higher negative pressure coefficient in the mid region of the body with 12 percent increase at the mid point. The convergence was achieved in 9 iterations with CPU time of 72 secs. Fig. 16 shows pressure distribution in free air for Mach numbers .7 and .8. The converged in 3 and 4 iterations respectively taking 23 secs and 31 secs of CPU time.

5.4 Conclusion

An integral equation approach has been described for numerically calculating inviscid subcritical transonic flow about slender bodies. It has also been demonstrated that the present technique can handle shock-free supercritical case. The accuracy of the results obtained by the present technique is almost of the same order as those obtained by relaxation procedures.

Calculations with wall boundary conditions have shown applicability of integral equation technique to the study of wind tunnel wall interference.

Further this technique can be applied to lifting problem.

REFERENCES

1. Ferrari, C. and Tricomi, F., 'Transonic Aerodynamics', Academic Press, 1968.
2. Oswatitsch, K., 'Die Geschwindigkeitsverteilung bei lokalen Überschallgezeiten an flachen Profilen', ZAMM, Vol. 30, pp. 17-24, 1950.
3. Gullstrand, T.R., 'The Flow over Symmetric Airfoils without Incidence in the lower Transonic Range', KTH Aero. TN 20, 1951.
4. Gullstrand, T.R., 'The Flow over symmetric Airfoils without Incidence at Transonic Speeds', KTH Aero TN 24, 1952.
5. Gullstrand, T.R., 'A Theoretical Discussion of some Properties of Transonic Flow over Two-dimensional Symmetrical Airfoils at Zero Lift with a simple method to Estimate the Flow Properties', KTH Aero. TN 25, 1952.
6. Gullstrand, T.R., 'The Flow over Two-Dimensional Airfoils at Incidence Transonic Speed Range', KTH Aero TN 27, 1952.
7. Gullstrand, T.R., 'Transonic Flow Past Two-Dimensional Airfoils', Zeitschrift für Flugwissenschaften, Vol.1, pp. 38-46, 1953.
8. Spreiter, J.P. and Alkane, A.Y., 'Theoretical Prediction of Pressure Distributions on Non-lifting Airfoils at High Subsonic Speed', NACA Report 1217, 1955.
9. Heaslet, M.A. and Spreiter, J.R., 'Three-Dimensional Transonic Flow Theory Applied to Slender Wings and Bodies', NACA Tech. Rep. 1318, 1956.
10. Nørstrud, H., 'Numerische Lösungen für Schallnahe Strömungen und Ebene Profile', Zeitschrift für Flugwissenschaften, Heft S, Vol.18, pp.149-157, 1970.
11. Nørstrud, H., 'The Transonic Airfoil Problem with Embedded Shocks', Aero. Quart., Vol. XXIV, Part 2, pp. 129-138, 1973.
12. Nørstrud, H., 'Transonic Flow Past Lifting Wings', AIAA J, Vol.11, No.5, pp. 754-757, 1973.

13. Nørstrud, H., 'High Speed Flow Past Wings', NASA CR- 2246, 1973.
14. Nixon, D. and Hancock, G.J., 'High Subsonic Flow Past a Steady Two-Dimensional Airfoils', ARC CP 1280, 1974.
15. Nixon, D., 'An Airfoil Oscillating at Low Frequency in a High Subsonic Flow', ARC CP 1285, 1974.
16. Nixon, D., 'Extended Integral Equation Method for Transonic Flows', AIAA J, Vol.13, No.7, pp.934, 1975.
17. Nixon, D., 'A Comparison of Two-Integral Equation Methods for High Subsonic Lifting Flows', Aero. Quart. Vol. XXVI, Part 1, pp. 56-58, 1975.
18. Sells, C.C.L., 'Plane Supercritical Flow Past a Lifting Airfoil, Proc. Roy. Soc., Ser.A., Vol.38 No. 1494, Jan. 1968.
19. Ogana, W., 'Numerical Solution for Subcritical Flows by a Transonic Integral Equation Method', AIAAJ, Vol.15, No.3, pp. 444-446, 1977.
20. Bailey, F.R., 'Numerical Calculation of Transonic Flow about Slender Bodies of Revolution', NASA TN - D 6582, 1971.
21. Murman, E.M., 'Computation of Wall Effects in Ventilated Transonic Wind Tunnels', AIAA paper 72-1007, AIAA 7th Aerodynamic Test Conference, Sept.1972.
22. Kacprzyński, J.J., 'Transonic Flow Past Two-Dimensional Airfoils between Porous Wind Tunnel Walls with Non-linear Characteristics', AIAA paper 75-81, AIAA 13th Aerospace Science Meeting, Jan.1975.
23. Newman, P.A. and Klucker, E.B., 'Numerical Modelling of Tunnel-Wall and Body Shape on Transonic Flow over Finite Lifting Wings', NASA SP 347, pp.1189-1212, 1975.
24. Murman, E.M., Bailey, F.R. and Johnson, M.L., 'TSFOIL - A Computer Code for Two-Dimensional Transonic Calculations, Including Wind-Tunnel Wall Effects and Wave-Drag Evaluation', NASA SP-347, pp. 769-782, 1975.

25. Kraft, E.M., 'An Integral Equation Method for Boundary Interference in a Perforated Wall Wind-Tunnel at Transonic Speeds,' AE DC - TR - 76-43, April 1976.
26. Goodman, T.R., 'The Porous Wall Wind Tunnel Part II -Interference Effects on a Cylindrical Body in a Two-Dimensional Tunnel at Subsonic Speed', Cornell Aeronautical Lab. Inc., Rep. AD- 594-A-3.
27. Ashley, H. and Landahl, M., 'Aerodynamics of Wings and Bodies,' Addison-Wesley Publishing Company Inc., Reading, Massachusetts.
28. Byrd, P.F. and Friedman, M.D., 'Handbook of Elliptic Integrals for Engineers and Scientists', Springer-Verlag Berlin, Heidelberg, New York 1971.
29. Taylor, R.A. and McDevitt, J.B., 'Pressure Distributions at Transonic Speeds for Parabolic Arc Bodies of Revolution Having Fineness Ratios of 10, 12 and 14', NACA TN- 4234 (1958).
30. Taylor, R.A. and McDevitt, J.B., 'Pressure Distribution at Transonic Speeds for Slender Bodies Having Various Axial Location of Maximum Diameter', NACA TN-4280 (1958).
31. Lock, R.C., 'Test Cases For Numerical Methods in Two-Dimensional Transonic Flows', AGARD-R-575-70.

APPENDIX AA-I Simplification of expression (3.11):-

Expression (3.11) is an integral over wall given by

$$\begin{aligned}
 I_{S_W} &= - \bar{r}_W \int_{-\infty}^{\infty} \int_0^{2\pi} \left(\psi \frac{p}{\bar{r}} \bar{\rho}_\xi + \bar{\rho} \psi_\rho \right)_{\rho = \bar{r}_W} dv d\xi \\
 &= - \frac{\bar{r}_W p}{\bar{r}} \int_{-\infty}^{\infty} \bar{\rho}_\xi \int_0^{2\pi} \psi dv d\xi - \bar{r}_W \int_{-\infty}^{\infty} \bar{\rho} \int_0^{2\pi} \psi_\rho dv d\xi \quad (A.1)
 \end{aligned}$$

Now consider each integral over v separately with $\psi = \frac{1}{4\pi \bar{R}}$;

$$\bar{R} = [(\bar{x} - \xi)^2 + \bar{r}^2 + \bar{r}_W^2 - 2\bar{r} \bar{r}_W \cos(\theta - v)]^{1/2}$$

Without loss of generality we take $\theta = 0$. Hence we obtain

$$\begin{aligned}
 \int_0^{2\pi} \psi dv &= \frac{1}{2\pi} \int_0^\pi \frac{dv}{\bar{R}} \\
 &= \frac{1}{\pi} \frac{F(\pi/2, k)}{\sqrt{(\bar{x} - \xi)^2 + (\bar{r}_W + \bar{r})^2}} \quad (A.2)
 \end{aligned}$$

$$\text{where } k = \sqrt{\frac{4\bar{r} \bar{r}_W}{(\bar{x} - \xi)^2 + (\bar{r} + \bar{r}_W)^2}}$$

(see 291.00 of reference [28])

Again,

$$\begin{aligned}
 \int_0^{2\pi} \psi_\rho dv &= - \frac{1}{4\pi} \int_0^{2\pi} \frac{\bar{r}_W - \bar{r} \cos v}{\bar{R}^3} dv \\
 &= - \frac{1}{2\pi} \left[(\bar{r}_W - \bar{r}) \int_0^\pi \frac{\partial v}{\bar{R}^3} + \bar{r} \int_0^\pi \frac{1 - \cos v}{\bar{R}^3} dv \right]
 \end{aligned}$$

$$\begin{aligned}
&= - \frac{1}{2\pi} \left[(\bar{r}_w - \bar{r}) \frac{2E(\pi/2, k)}{\sqrt{(\bar{x}-\xi)^2 + (\bar{r}_w + \bar{r})^2} \left[(\bar{x}-\xi)^2 + (\bar{r}_w - \bar{r})^2 \right]} \right. \\
&\quad \left. + \frac{1}{\bar{r}_w} \frac{F(\pi/2, k) - E(\pi/2, k)}{\sqrt{(\bar{x}-\xi)^2 + (\bar{r}_w + \bar{r})^2}} \right] \quad (A.3)
\end{aligned}$$

(see 291.01 and 291.06 of reference [28])

Hence expression (A.1) leads to :

$$\begin{aligned}
I_{S_w} &= \int_{-\infty}^{\infty} \left[(\bar{r}_w - \bar{r}) \frac{E(\pi/2, k)}{\left[(\bar{x}-\xi)^2 + (\bar{r}_w - \bar{r})^2 \right] \sqrt{(\bar{x}-\xi)^2 + (\bar{r}_w + \bar{r})^2}} \right. \\
&\quad \left. + \frac{1}{2\pi} \frac{F(\pi/2, k) - E(\pi/2, k)}{\sqrt{(\bar{x}-\xi)^2 + (\bar{r}_w + \bar{r})^2}} \right) \bar{\phi}(\xi, \bar{r}_w) \\
&\quad \left. - \frac{p}{\beta} \frac{\bar{r}_w}{\pi} \frac{E(\pi/2, k)}{\sqrt{(\bar{x}-\xi)^2 + (\bar{r}_w + \bar{r})^2}} \right] d\xi \quad (A.4)
\end{aligned}$$

A-II Differentiation of equation (3.19) w.r.t. \bar{x} :

The differentiation of equation (3.19) w.r.t. \bar{x} is straight forward except the wall integral term

$$I_{S_w} = \int_{-\infty}^{\infty} \left[(A+B) \bar{\phi}(\xi, \bar{r}_w) - \frac{p}{\beta} \bar{\phi}_{\xi}(\xi, \bar{r}_w) \right] d\xi \quad (A.5)$$

On differentiating (A.5) w.r.t. \bar{x} , we have

$$\begin{aligned}
\frac{\partial I_{S_w}}{\partial \bar{x}} &= \int_{-\infty}^{\infty} \left[\bar{\phi} \frac{\partial}{\partial \bar{x}} (A+B) - \frac{p}{\beta} \bar{\phi} \frac{\partial G}{\partial \bar{x}} \right] d\xi \\
&= \int_{-\infty}^{\infty} \left[\bar{\phi} \frac{\partial}{\partial \xi} (A+B) - \frac{p}{\beta} \bar{\phi}_{\xi} \frac{\partial G}{\partial \xi} \right] d\xi \quad \left[\begin{array}{l} \text{Since } \frac{\partial f(\bar{x}-\xi)}{\partial \bar{x}} \\ = -\frac{\partial f(\bar{x}-\xi)}{\partial \xi} \end{array} \right]
\end{aligned}$$

$$\begin{aligned}
 \text{here } \frac{\partial G}{\partial \xi} &= \frac{\partial}{\partial \xi} \left[\frac{\bar{r}_w F(\pi/2, k)}{\pi \sqrt{(\bar{x}-\xi)^2 + (\bar{r}_w + \bar{r})^2}} \right] \\
 &= \frac{\bar{r}_w}{\pi} \frac{(\bar{x}-\xi) E(\pi/2, k)}{[(\bar{x}-\xi)^2 + (\bar{r}_w - \bar{r})^2] \sqrt{(\bar{x}-\xi)^2 + (\bar{r}_w + \bar{r})^2}}
 \end{aligned}$$

(see 710.00 of reference [28])

Hence

$$\begin{aligned}
 \frac{\partial I_{S_w}}{\partial \bar{x}} &= - \left[\bar{\phi}(A+B) \Big|_{\xi=-\infty}^{\xi=+\infty} - \int_{-\infty}^{\infty} (A+B) \bar{\phi}_{\xi} d\xi \right. \\
 &\quad \left. - \frac{\bar{r}_w}{\pi} \frac{(\bar{x}-\xi) E(\pi/2, k)}{[(\bar{x}-\xi)^2 + (\bar{r}_w - \bar{r})^2] \sqrt{(\bar{x}-\xi)^2 + (\bar{r}_w + \bar{r})^2}} \right] \\
 &= \int_{-\infty}^{\infty} (A+B+D) \bar{u}(\xi, \bar{r}_w) d\xi \tag{A.6}
 \end{aligned}$$

APPENDIX B

To deduce expression (3.32):

We have wall integral

$$\begin{aligned}
 I_{C_T} &= \delta \int_{C_T} (\bar{\phi} \psi_n - \psi \bar{\phi}_n) dG \\
 &\quad \text{at wall} \\
 &= \delta \left[\int_{-\infty}^{\infty} (\bar{\phi} \psi_n - \psi \bar{\phi}_n) dG \right]_{\zeta=\bar{y}_W} + \int_{-\infty}^{\infty} (\bar{\phi} \psi_n - \psi \bar{\phi}_n) dG \Big|_{\zeta=-\bar{y}_W}
 \end{aligned}
 \tag{B.1}$$

Since at $\zeta = \pm \bar{y}_W$, $\frac{\partial}{\partial n} = \mp \frac{\partial}{\partial \zeta}$

We have:

$$I_{C_T} = \delta \left[- \int_{-\infty}^{\infty} (\bar{\phi} \psi_{\zeta} - \psi \bar{\phi}_{\zeta}) \Big|_{\zeta=\bar{y}_W} d\xi + \int_{-\infty}^{\infty} (\bar{\phi} \psi_{\zeta} - \psi \bar{\phi}_{\zeta}) \Big|_{\zeta=-\bar{y}_W} d\xi \right]
 \tag{B.2}$$

Applying wall boundary condition (3.26) we get :

$$\begin{aligned}
 I_{C_T} &= \delta \left[- \int_{-\infty}^{\infty} (\bar{\phi} \psi_{\zeta} + \psi \frac{p}{\beta} \bar{\phi}_{\xi}) \Big|_{\zeta=\bar{y}_W} d\xi + \int_{-\infty}^{\infty} (\bar{\phi} \psi_{\zeta} - \psi \frac{p}{\beta} \bar{\phi}_{\xi}) \Big|_{\zeta=-\bar{y}_W} d\xi \right] \\
 &= - \delta \int_{-\infty}^{\infty} \left\{ \frac{p}{\beta} \bar{\phi}_{\xi}(\xi, \bar{y}_W) \left[\psi(\zeta=\bar{y}_W) + \psi(\zeta=-\bar{y}_W) \right] \right. \\
 &\quad \left. + \bar{\phi}(\xi, \bar{y}_W) \left[\psi_{\zeta}(\zeta=\bar{y}_W) - \psi_{\zeta}(\zeta=-\bar{y}_W) \right] \right\} d\xi
 \end{aligned}
 \tag{B.3}$$

(since $\bar{\phi}$ and $\bar{\phi}_{\xi}$ are symmetric about ζ -axis)

Now integrating by parts the second expression in above integral and applying boundary condition (3,25) we get :

$$\begin{aligned}
 I_{O_T} = & -\delta \int_{-\infty}^{\infty} \bar{\partial}_{\xi} (\xi, \bar{y}_w) \left\{ \frac{\partial}{\partial \xi} [\psi(\xi = \bar{y}_w) - \psi(\xi = -\bar{y}_w)] \right. \\
 & \left. - \int [\psi_{\xi}(\xi = \bar{y}_w) - \psi_{\xi}(\xi = -\bar{y}_w)] d\xi \right\} d\xi
 \end{aligned}
 \tag{B.4}$$

APPENDIX C

To simplify b_{iwSP} of expression (4.4) :

$$b_{iwSP} = \int_{\bar{x}_i - \delta_i}^{\bar{x}_i + \delta_i} (A+B+D) d\xi \quad (C.1)$$

Integrating each term on R.H.S. separately:

$$\int_{\bar{x}_i - \delta_i}^{\bar{x}_i + \delta_i} A d\xi = \frac{\bar{r}_w(\bar{r}_w - \bar{r}_p)}{\pi} E(\pi/2, k_{\bar{x}_i}) \int_{\bar{x}_i - \delta_i}^{\bar{x}_i + \delta_i} \frac{d\xi}{(a-b)\bar{a}^{1/2}}$$

$$\text{with } a = (\bar{x}_S - \xi)^2 + (\bar{r}_p + \bar{r}_w)^2 ; b = 4 \bar{r}_p \bar{r}_w \quad (C.2)$$

$$\text{and } k_{\bar{x}_i} = (b/a)^{1/2}_{\xi=\bar{x}_i} = \sqrt{\frac{4 \bar{r}_p \bar{r}_w}{(\bar{x}_S - \bar{x}_i)^2 + (\bar{r}_p + \bar{r}_w)^2}}$$

Taking $k_{\bar{x}_i}$ constant over the small interval $\bar{x}_i - \delta_i \leq \xi \leq \bar{x}_i + \delta_i$ so that $E(\pi/2, k_{\bar{x}_i})$ becomes constant over that interval, hence (C.2) gives

$$\begin{aligned} \int_{\bar{x}_i - \delta_i}^{\bar{x}_i + \delta_i} A d\xi &= \sqrt{\frac{\bar{r}_w}{\bar{r}_p}} \frac{E(\pi/2, k_{\bar{x}_i})}{2\pi} \left[\tan^{-1} \frac{\bar{x}_i + \delta_i - \bar{x}_S}{(\bar{r}_w - \bar{r}_p)} k_{\bar{x}_i + \delta_i} \right. \\ &\quad \left. - \tan^{-1} \frac{\bar{x}_i - \delta_i - \bar{x}_S}{\bar{r}_w - \bar{r}_p} k_{\bar{x}_i - \delta_i} \right] \quad (C.3) \end{aligned}$$

Similarly $\int_{\bar{x}_i - \delta_i}^{\bar{x}_i + \delta_i} B d\xi = \frac{[F(\pi/2, k_{\bar{x}_i}^-) - E(\pi/2, k_{\bar{x}_i}^-)]}{2\pi}$

$$\ln \frac{\bar{x}_i + \delta_i - \bar{x}_S + \sqrt{(\bar{x}_i + \delta_i - \bar{x}_S)^2 + (\bar{r}_W + \bar{r}_P)^2}}{\bar{x}_i - \delta_i - \bar{x}_S + \sqrt{(\bar{x}_i - \delta_i - \bar{x}_S)^2 + (\bar{r}_W + \bar{r}_P)^2}} \quad (0.4)$$

where $F(\pi/2, k_{\bar{x}_i}^-)$ and $E(\pi/2, k_{\bar{x}_i}^-)$ are assumed constant over the small interval and

$$\int_{\bar{x}_i - \delta_i}^{\bar{x}_i + \delta_i} D d\xi = -\frac{p}{4\pi\beta} \sqrt{\frac{\bar{r}_W}{\bar{r}_P}} E(\pi/2, k_{\bar{x}_i}^-) \ln \frac{1-k_{\bar{x}_i+\delta_i}^-}{1+k_{\bar{x}_i+\delta_i}^-} \frac{1+k_{\bar{x}_i-\delta_i}^-}{1-k_{\bar{x}_i-\delta_i}^-} \quad (0.5)$$

Combining (0.3), (0.4), (0.5) in (0.1), we obtain

$$b_{iwSP} = \frac{E(\pi/2, k_{\bar{x}_i}^-)}{2\pi} \sqrt{\frac{\bar{r}_W}{\bar{r}_P}} \left[\tan^{-1} \frac{X_1}{(\bar{r}_W - \bar{r}_P)} k_{\bar{x}_i - \delta_i}^- \right. \\ \left. - \tan^{-1} \frac{X_2}{\bar{r}_W - \bar{r}_P} k_{\bar{x}_i + \delta_i}^- - \frac{p}{2\beta} \ln \frac{1-k_{\bar{x}_i+\delta_i}^-}{1+k_{\bar{x}_i+\delta_i}^-} \frac{1+k_{\bar{x}_i-\delta_i}^-}{1-k_{\bar{x}_i-\delta_i}^-} \right] \\ + \frac{F(\pi/2, k_{\bar{x}_i}^-) - E(\pi/2, k_{\bar{x}_i}^-)}{2\pi} \ln \frac{\sqrt{X_2^2 + (\bar{r}_W + \bar{r}_P)^2} - X_2}{\sqrt{X_1^2 + (\bar{r}_W + \bar{r}_P)^2} - X_1}$$

where $X_1 = \bar{x}_S - \bar{x}_i + \delta_i$ (0.6)

$X_2 = \bar{x}_S - \bar{x}_i - \delta_i$

APPENDIX D

To deduce expression (4.7) :

$$a_{ijSP} = \frac{1}{2} \int_{\bar{r}_j - q_j}^{\bar{r}_j + h_j} \int_0^{2\pi} \int_{\bar{x}_i - \delta_i}^{\bar{x}_i + \delta_i} \psi_{\xi \bar{x}} \rho d\xi dv d\rho \quad (D.1)$$

Integrating R.H.S . w.r.t. ξ we get:

$$\begin{aligned} a_{ijSP} &= \frac{1}{2} \int_{\bar{r}_j - q_j}^{\bar{r}_j + h_j} \int_0^{2\pi} [\psi_{\bar{x}}]_{\bar{x}_i - \delta_i}^{\bar{x}_i + \delta_i} \rho dv d\rho \\ &= \frac{1}{8\pi} \int_{\bar{r}_j - q_j}^{\bar{r}_j + h_j} \int_0^{2\pi} \left[\frac{X_1}{(X_1^2 + \bar{r}_P^2 + \rho^2 - 2\bar{r}_P \rho \cos v)^{3/2}} \right. \\ &\quad \left. - \frac{X_2}{(X_2^2 + \bar{r}_P^2 + \rho^2 - 2\bar{r}_P \rho \cos v)^{3/2}} \right] \rho dv d\rho \end{aligned} \quad (D.2)$$

where $X_1 = \bar{x}_S - \bar{x}_i + \delta_i$

$X_2 = \bar{x}_S - \bar{x}_i - \delta_i$

Further we have :

$$I = \int_{\bar{r}_j - q_j}^{\bar{r}_j + h_j} \int_0^{2\pi} \frac{X}{(X^2 + \bar{r}_P^2 + \rho^2 - 2\bar{r}_P \rho \cos v)^{3/2}} \rho dv d\rho$$

$$\begin{aligned}
&= \int_{\bar{r}_j - q_j}^{\bar{r}_j + h_j} 2X \int_0^\pi \frac{dv \rho d\rho}{[X^2 + \bar{r}_p^2 + \rho^2 - 2\bar{r}_p \rho \cos v]}^{3/2} \\
&= \int_{\bar{r}_j - q_j}^{\bar{r}_j + h_j} \frac{4X E(\pi/2, k)}{\sqrt{X^2 + (\bar{r}_p + \rho)^2} [X^2 + (\bar{r}_p - \rho)^2]} d\rho \quad (D.3)
\end{aligned}$$

(see 291.04 of reference [28])

where $k = \sqrt{\frac{4\bar{r}_p}{X^2 + (\bar{r}_p + \rho)^2}}$

$E(\pi/2, k)$ is complete elliptic integral of second kind. Further within the accuracy of numerical computation we take

$$\frac{\rho}{\sqrt{X^2 + (\bar{r}_p + \rho)^2}} E(\pi/2, k)$$

constant over interval $\bar{r}_j - q_j \leq \rho \leq \bar{r}_j + h_j$ with $\rho = \bar{r}_j$ as the point of constancy. We obtain

$$\begin{aligned}
I &= \frac{4X \bar{r}_j}{\sqrt{X^2 + (\bar{r}_p + \bar{r}_j)^2}} E(\pi/2, k(X)) \int_{\bar{r}_j - q_j}^{\bar{r}_j + h_j} \frac{d\rho}{[X^2 + (\bar{r}_p - \rho)^2]} \\
&= \frac{4\bar{r}_j}{\sqrt{X^2 + (\bar{r}_j + \bar{r}_p)^2}} E(\pi/2, k(X)) \left[\tan^{-1} \frac{\bar{r}_j + h_j - \bar{r}_p}{X} \right. \\
&\quad \left. - \tan^{-1} \frac{\bar{r}_j - q_j - \bar{r}_p}{X} \right] \quad (D.4)
\end{aligned}$$

$$\text{where } k(X) = \sqrt{\frac{4\bar{r}_P \bar{r}_j}{X^2 + (\bar{r}_P + \bar{r}_j)^2}}$$

Finally using (D.4) in (D.2) we obtain

$$a_{ijSP} = \frac{1}{2\pi} \left[G(X_1) E(\pi/2, k(X_1)) T(X_1) \right. \\ \left. - G(X_2) E(\pi/2, k(X_2)) T(X_2) \right]$$

APPENDIX E

I. Evaluation of $u_L(\bar{x}, \bar{r})$ for general parabolic body of revolution :

The equation for profile of general parabolic body of revolution is given by following two equations.

The body for which maximum thickness lies forward of its mid-point :

$$R = C R_{\max} [1 - \xi - (1-\xi)^n] \quad (E.1)$$

The body for which maximum thickness lies aft of its mid point :

$$R = C R_{\max} (\xi - \xi^n) \quad (E.2)$$

The following table gives the data for various C and n combinations with position of maximum thickness:

ξ (for max thick- ness)	C	n	R (the formula used)
0.3	1.71	6.03	(E.1)
0.4	2.36	3.39	(E.1)
0.5	4.00	2.00	(E.1) or (E.2)
0.6	2.36	3.39	(E.2)
0.7	1.71	6.03	(E.2)

(see reference [30])

The value of $u_L(\bar{x}, \bar{r})$ can be calculated using equations (4.2) and (4.3) with l being location of sting ($l = 1$ for no sting). However integral in equation (4.2) can be evaluated analytically for bodies having maximum thickness at mid-point.

The profile is given by :

$$R = 4 R_{\max} (\xi - \xi^2)$$

hence

$$S(\xi) = 16\pi R_{\max}^2 (\xi - \xi^2)^2$$

$$S'(\xi) = 32\pi R_{\max}^2 (2\xi^3 - 3\xi^2 + \xi)$$

$$S''(\xi) = 32\pi R_{\max}^2 (6\xi^2 - 6\xi + 1)$$

We put these values in equation (4.2) and evaluate the integral of equation (4.2) as follows:

$$\begin{aligned} \int_0^l \frac{S''(\bar{x}) - S''(\xi)}{|\bar{x} - \xi|} d\xi &= 192\pi R_{\max}^2 \int_0^l \frac{\bar{x}^2 - \xi^2(\bar{x} - \xi)}{|\bar{x} - \xi|} d\xi \\ &= 192\pi R_{\max}^2 \int_0^l \frac{\bar{x} - \xi}{|\bar{x} - \xi|} (\bar{x} + \xi - 1) d\xi \\ &= I \end{aligned}$$

Now three cases arise

i) for $\bar{x} < 0$

$$I = 192\pi R_{\max}^2 l \left(1 - \bar{x} - \frac{l}{2} \right)$$

ii) for $0 \leq x \leq l$:

$$I = 192\pi R_{\max}^2 \left[3\bar{x}^2 - 2(\bar{x} + l) - \frac{l^2}{2} + l \right]$$

and iii) for $x \geq l$

$$I = 192\pi R_{\max}^2 l \left[\bar{x} + \frac{l}{2} - 1 \right]$$

II. Evaluation of $u_L(\bar{x}, \bar{y})$ for parabolic airfoils and NACA OOX airfoils :

For parabolic airfoil the upper airfoil profile is defined by

$$Y_+(\xi) = 2\tau(\xi - \xi^2)$$

where τ is thickness ratio of airfoil.

Putting it in equation (3.38) we get

$$\begin{aligned} u_L(\bar{x}, \bar{y}) &= \frac{1}{\pi\beta} \int_0^1 \frac{\bar{x} - \xi}{[(\bar{x} - \xi)^2 + \bar{y}^2]} 2\tau(1 - 2\xi) d\xi \\ &= \frac{2\tau}{\pi\beta} \left[(2\xi - 1) \ln [(\bar{x} - \xi)^2 + \bar{y}^2]^{1/2} d\xi \right]_0^1 \\ &\quad - 2 \int_0^1 \ln [(\bar{x} - \xi)^2 + \bar{y}^2]^{1/2} d\xi \\ &= \frac{2\tau}{\pi\beta} \left\{ \ln [(\bar{x} - 1)^2 + \bar{y}^2]^{1/2} [\bar{x}^2 + \bar{y}^2]^{1/2} \right. \\ &\quad - [(\xi - \bar{x}) \ln [(\bar{x} - \xi)^2 + \bar{y}^2] - 2(\xi - \bar{x}) \\ &\quad \left. + 2\bar{y} \tan^{-1} \frac{\xi - \bar{x}}{\bar{y}}] \right\}_0^1 \\ &= \frac{2\tau}{\pi\beta} \left(\frac{1}{2} - \bar{x} \right) \ln \frac{\bar{x}^2 + \bar{y}^2}{(1 - \bar{x})^2 + \bar{y}^2} + 2 \\ &\quad - 2\bar{y} \left[\tan^{-1} \frac{1 - \bar{x}}{\bar{y}} + \tan^{-1} \frac{\bar{x}}{\bar{y}} \right] \end{aligned} \quad (E.3)$$

Similarly for NACA 00XX airfoil we have :

$$Y_+(\xi) = B_1 \sqrt{\xi} + B_2 \xi + B_4 \xi^2 + B_6 \xi^3 + B_8 \xi^4$$

where B_1, B_2, B_4, B_6 and B_8 are constants

hence

$$\frac{dY_+(\xi)}{d\xi} = \left[\frac{B_1}{2\sqrt{\xi}} + B_2 + 2B_4\xi + 3B_6\xi^2 + 4B_8\xi^3 \right] \quad (E.4)$$

First we shall determine the $u_L(\bar{x}, \bar{y})$ on the surface of the body . Since airfoil is quite thin we can take the linear velocity perturbation on the surface as linear velocity perturbation on the axis $\bar{y} = 0$. So equation (3.37) becomes:

$$u_L(\bar{x}, 0^+) = \frac{1}{\pi\beta} \int_0^1 \frac{1}{\bar{x}-\xi} \frac{dY_+(\xi)}{d\xi} d\xi$$

Using (E.2) we get

$$u_L(\bar{x}, 0^+) = \frac{1}{\pi\beta} \int_0^1 \frac{1}{\bar{x}-\xi} \left[\frac{B_1}{2\sqrt{\xi}} + B_2 + 2B_4\xi + 3B_6\xi^2 + 4B_8\xi^3 \right] d\xi \quad (E.5)$$

Integrating (E.3) term by term :

$$\begin{aligned} \int_0^1 \frac{B_1}{2(\bar{x}-\xi)\sqrt{\xi}} d\xi &= B_1 \int_0^1 \frac{dt}{(\bar{x}-t^2)} \quad \text{where } t^2 = \xi \\ &= \frac{B_1}{2\sqrt{\bar{x}}} \ln \frac{1+\sqrt{\bar{x}}}{1-\sqrt{\bar{x}}} \end{aligned}$$

$$\int_0^1 \frac{B_2}{\bar{x}-\xi} d\xi = B_2 \ln \frac{\bar{x}}{1-\bar{x}}$$

$$\begin{aligned} \int_0^1 \frac{2B_4 \xi}{(\bar{x} - \xi)} d\xi &= 2B_4 \int_0^1 \left(-1 + \frac{\bar{x}}{\bar{x} - \xi} \right) d\xi \\ &= 2B_4 \left[-1 + \bar{x} \ln \frac{\bar{x}}{1 - \bar{x}} \right] \end{aligned}$$

$$\begin{aligned} \int_0^1 \frac{3B_6 \xi^2}{(\bar{x} - \xi)} d\xi &= 3B_6 \int_0^1 \left[-(\bar{x} + \xi) + \frac{\bar{x}}{\bar{x} - \xi} \right] d\xi \\ &= 3B_6 \left[-\frac{1}{2} - \bar{x} + \bar{x}^2 \ln \frac{\bar{x}}{1 - \bar{x}} \right] \end{aligned}$$

and

$$\begin{aligned} \int_0^1 \frac{4B_8 \xi^3}{(\bar{x} - \xi)} d\xi &= 4B_8 \int_0^1 \left[-(\xi^2 + \bar{x}\xi + \bar{x}^2) + \frac{\bar{x}^3}{\bar{x} - \xi} \right] d\xi \\ &= 4B_8 \left[-\frac{1}{3} - \frac{\bar{x}}{2} - \bar{x}^2 + \bar{x}^3 \ln \frac{\bar{x}}{1 - \bar{x}} \right] \end{aligned}$$

Hence (E.3) gives :

$$\begin{aligned} u_L(\bar{x}, 0^+) &= \frac{\tau}{\pi \beta} \left[\frac{B_1}{2\sqrt{\bar{x}}} \ln \frac{1 + \sqrt{\bar{x}}}{1 - \sqrt{\bar{x}}} - 2B_4 + \right. \\ &\quad \ln \frac{\bar{x}}{1 - \bar{x}} (B_2 + 2B_4 \bar{x} + 3B_6 \bar{x}^2 + 4B_8 \bar{x}^3) \\ &\quad \left. - 3B_6 \left(\frac{1}{2} + \bar{x} \right) + 4B_8 \left(\frac{1}{3} + \frac{\bar{x}}{2} + \bar{x}^2 \right) \right] \end{aligned} \quad (E.6)$$

The above solution for linear perturbation velocity on the plane of airfoil has square root and logarithmic singularities at the leading edge ($\bar{x} = 0$) which gives inaccurate results near the leading edge. It is modified by using following formula¹⁴ :

$$u_L^*(\bar{x}, 0^+) = \frac{1 + u_L(\bar{x}, 0^+)}{\left(1 + \left[\frac{1}{\beta} \frac{dY_+(\bar{x})}{d\bar{x}} \right]^2 \right)^{1/2}} - 1 \quad (E.7)$$

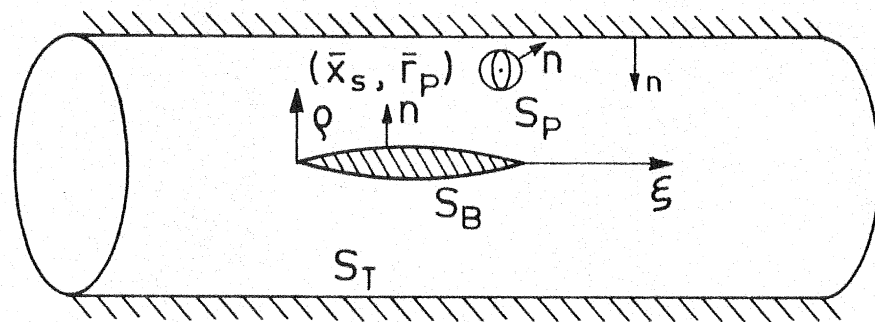


FIG. 1 SLENDER BODY IN AXISSYMMETRIC FLOW.

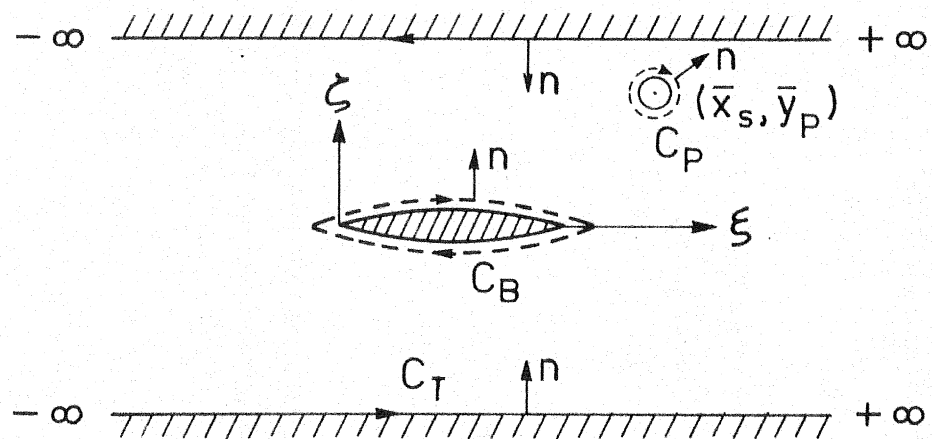
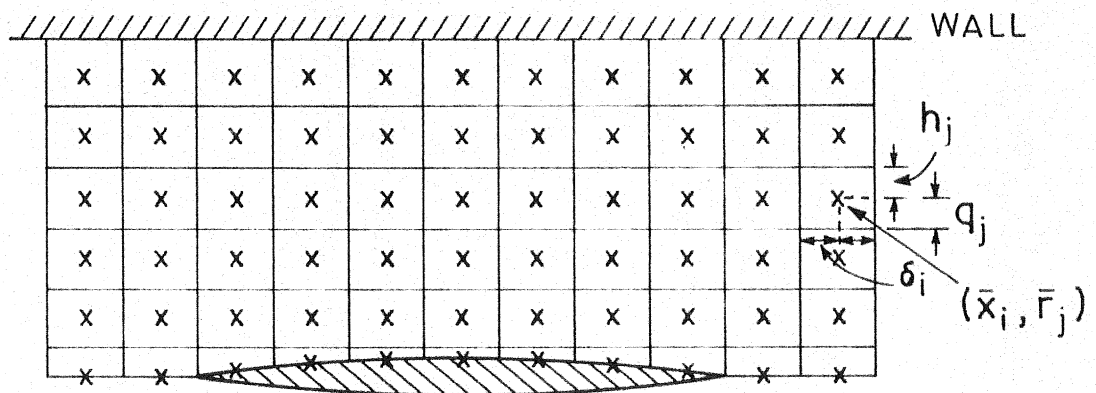
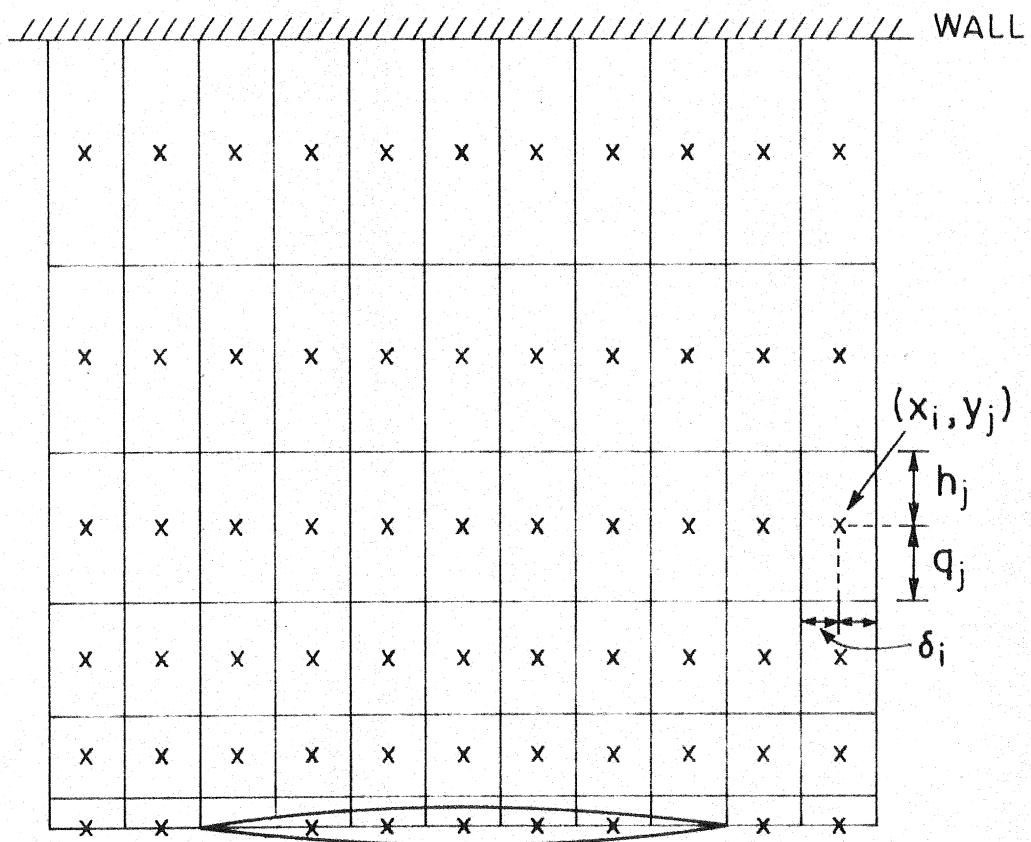


FIG. 2 THIN AIR FOIL IN TWO-DIMENSIONAL FLOW.



3 LOCATION OF GRID POINT IN RECTANGULAR ELEMENTS (axisymmetric flow).



4 LOCATION OF GRID POINT IN RECTANGULAR ELEMENTS (two-dimensional flow).

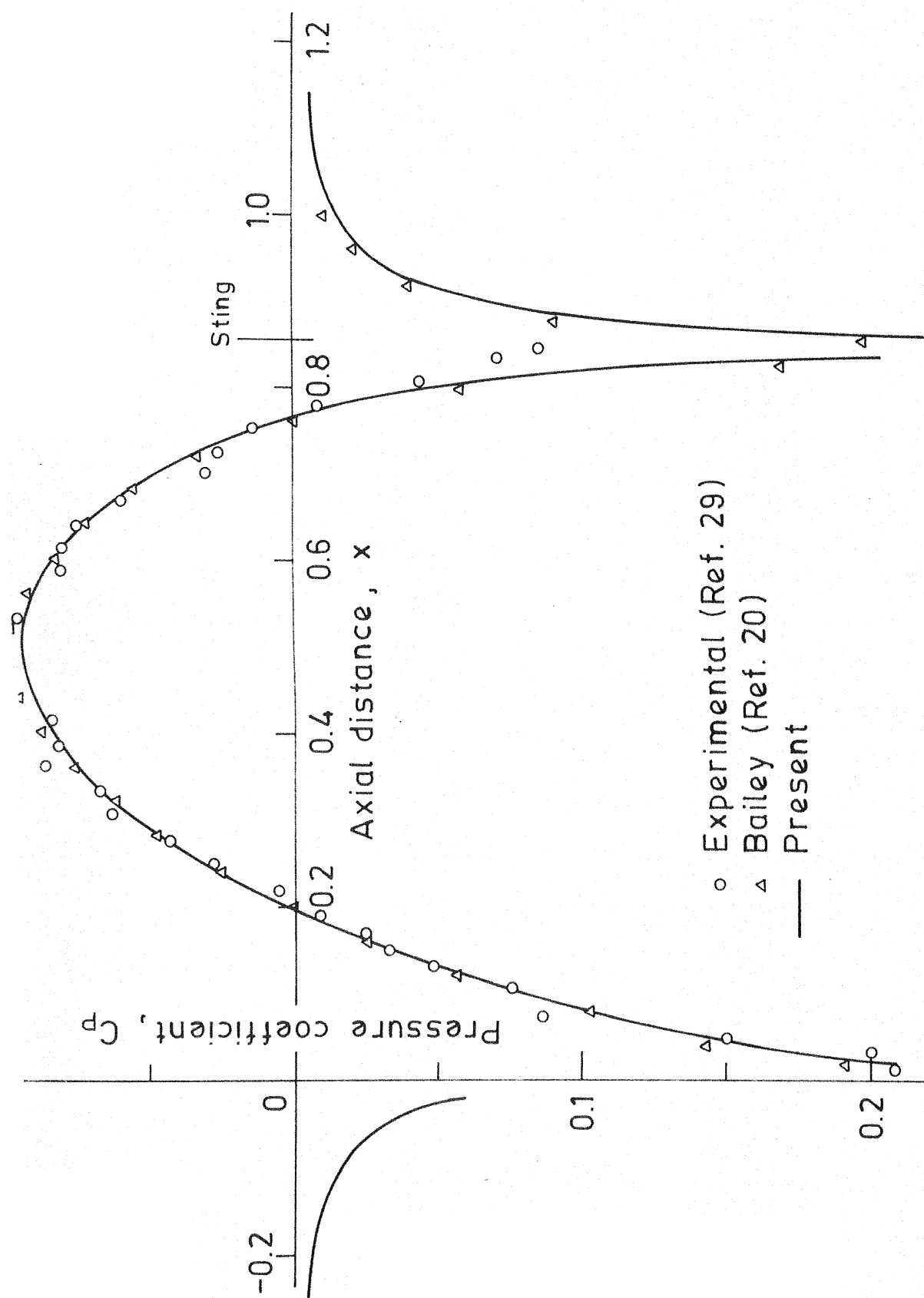


FIG. 5 DISTRIBUTION OF C_p ON PARABOLIC ARC OF REVOLUTION ($M_\infty = 0.9$, $FR = 10$, free air case).

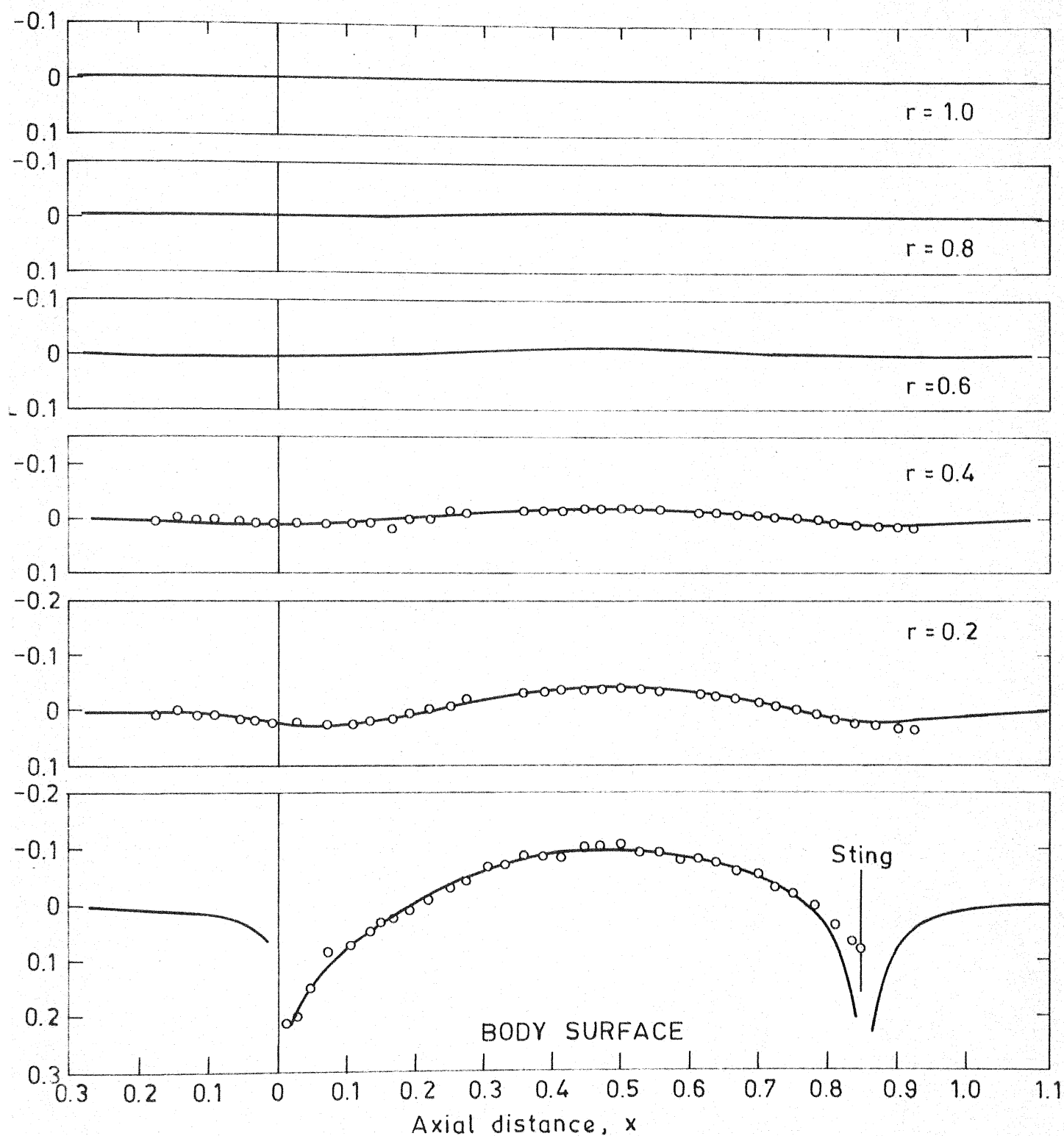


FIG. 6 DISTRIBUTION OF C_p FOR PARABOLIC ARC OF REVOLUTION ($M_\infty = 0.90$, $FR = 10$, free air case).

○ Experimental (Ref. 29) — Present

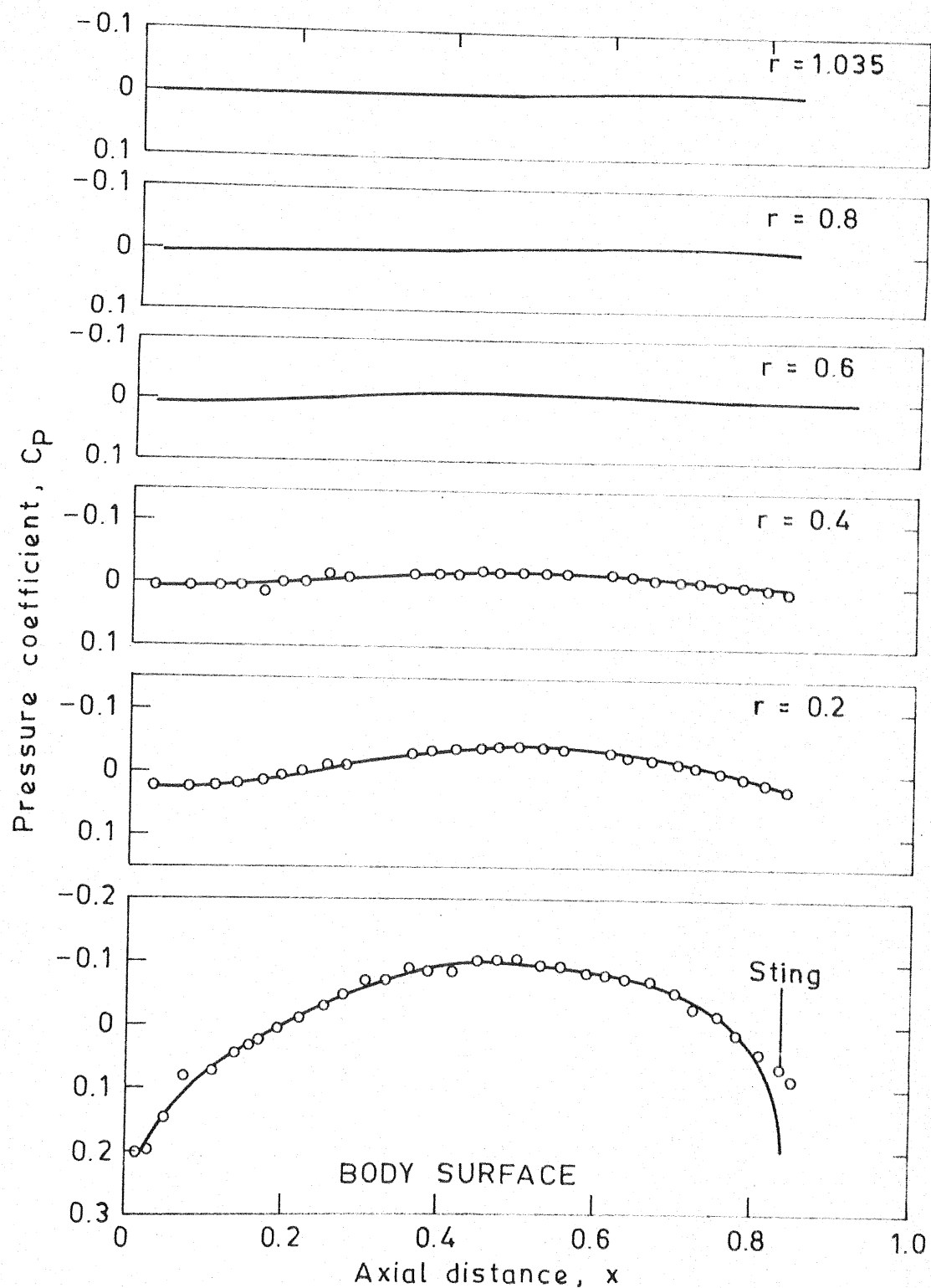


FIG. 7 DISTRIBUTION OF C_p FOR PARABOLIC ARC OF REVOLUTION ($M_\infty = 0.9$, $FR = 10$, wall interference case with porosity parameter = 0.77 and wall radius = 1.17).

○ Experimental (Ref. 29) — Present

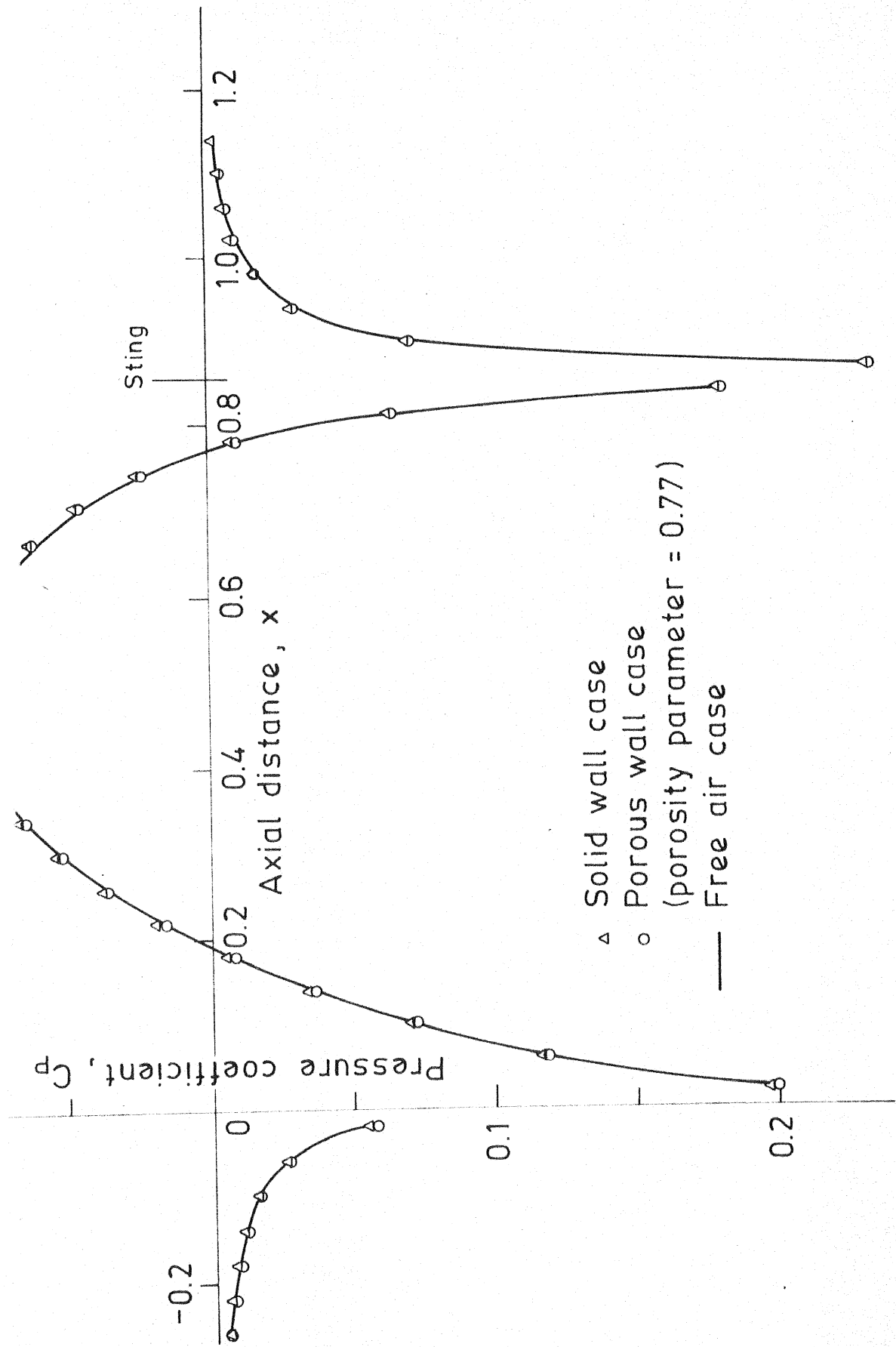


FIG. 8 DISTRIBUTION OF C_p ON PARABOLIC ARC OF REVOLUTION ($M_\infty = 0.85$, $FR = 10$, wall radius = 1.17).

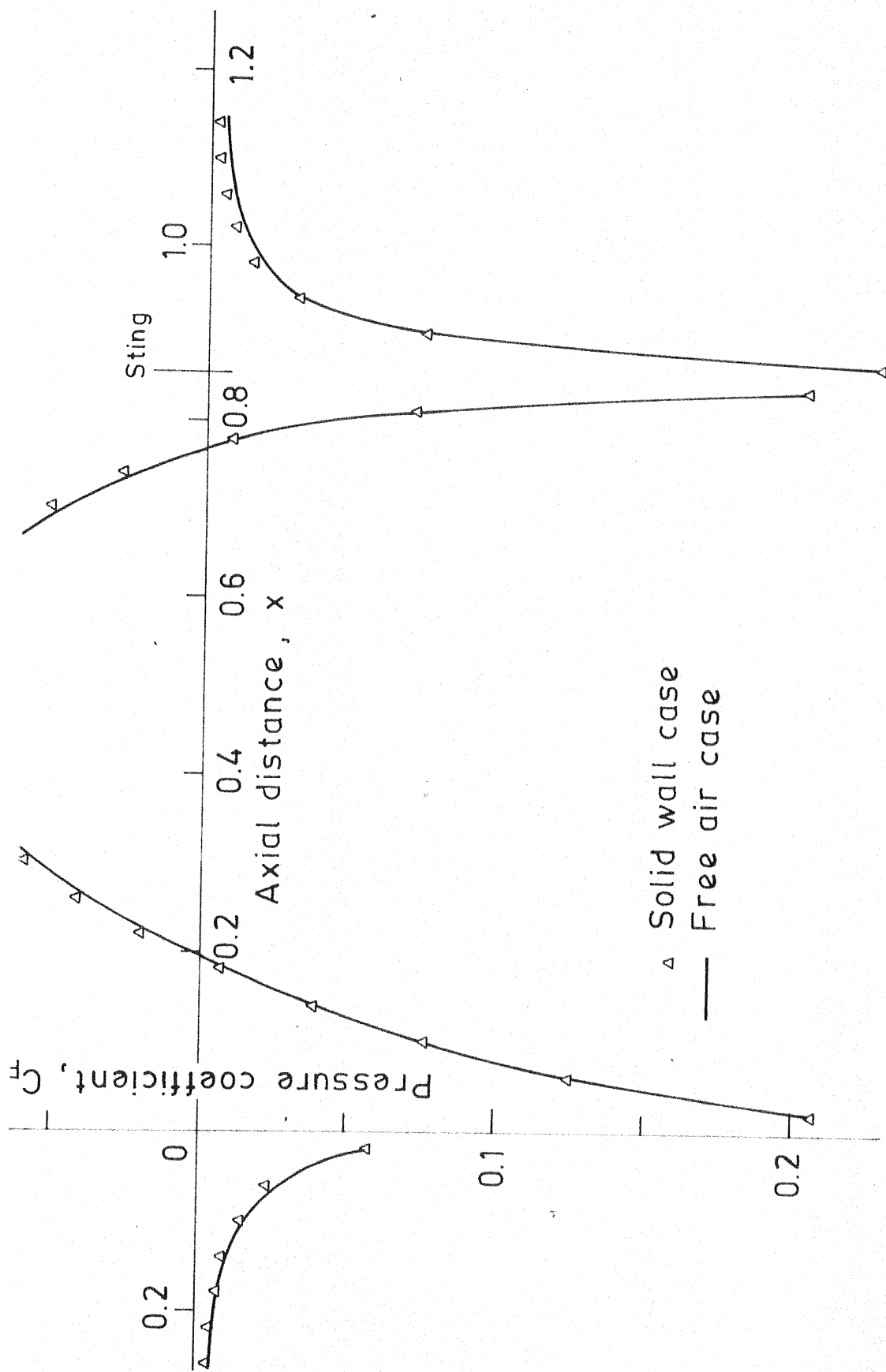
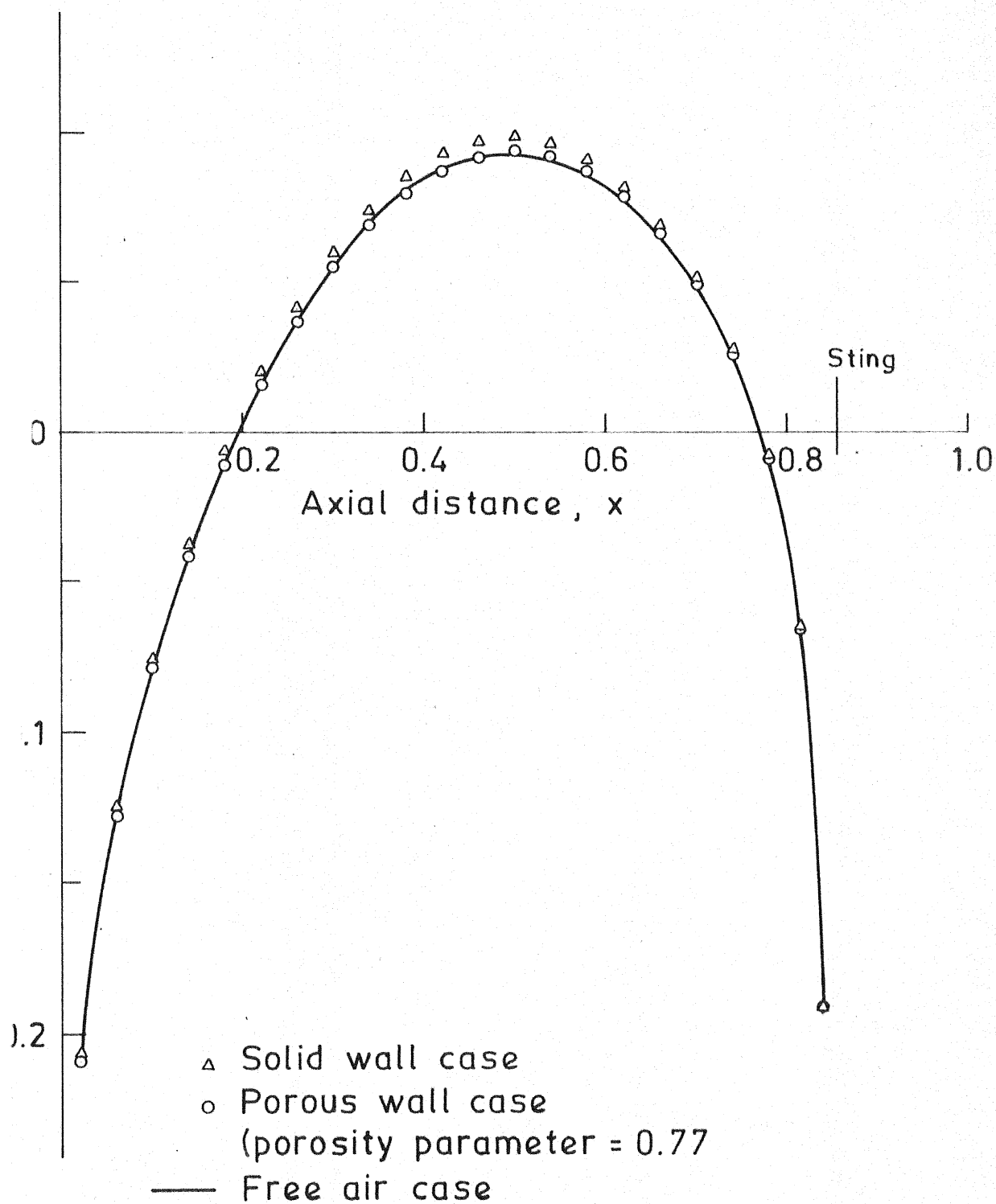
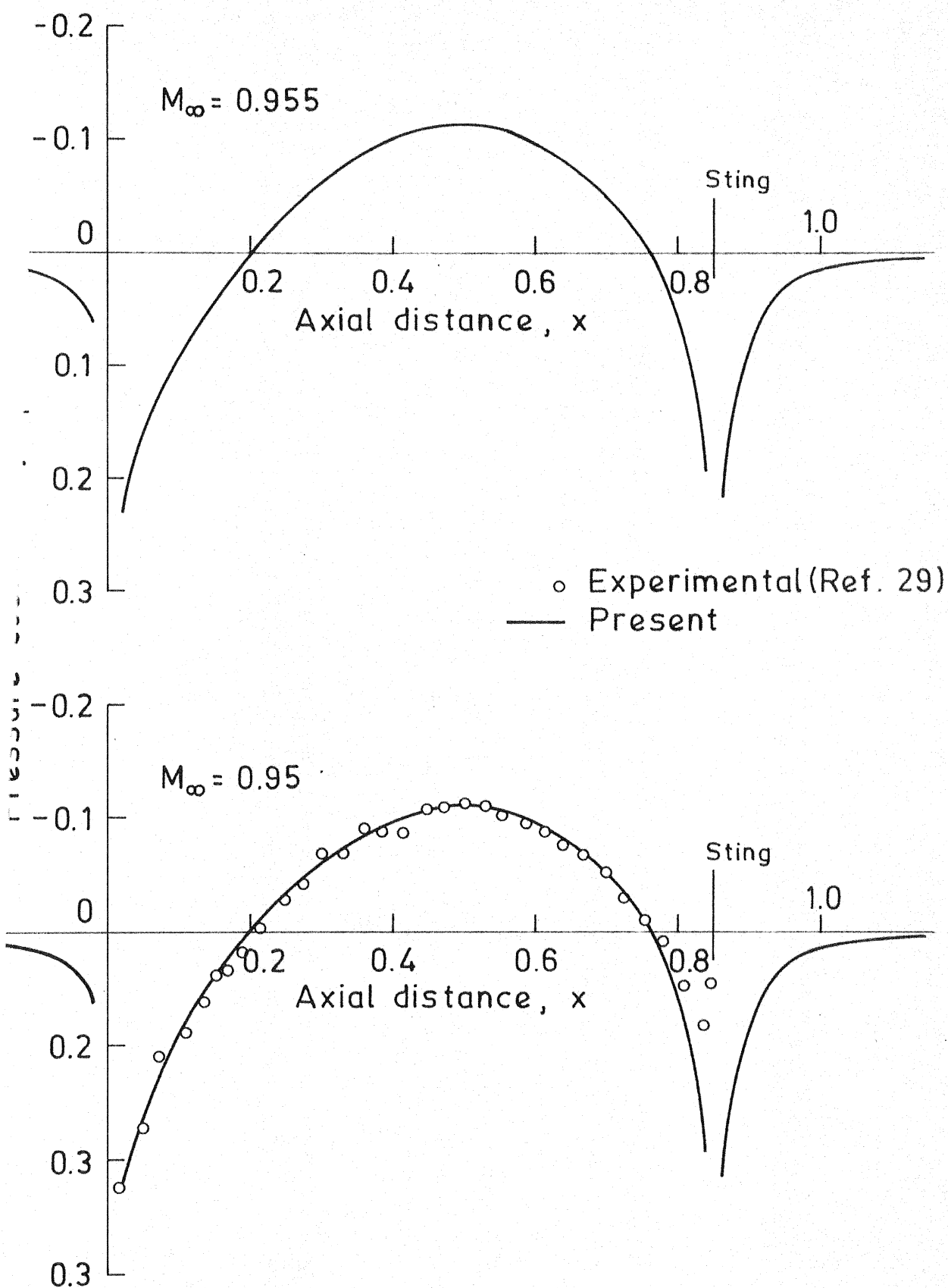


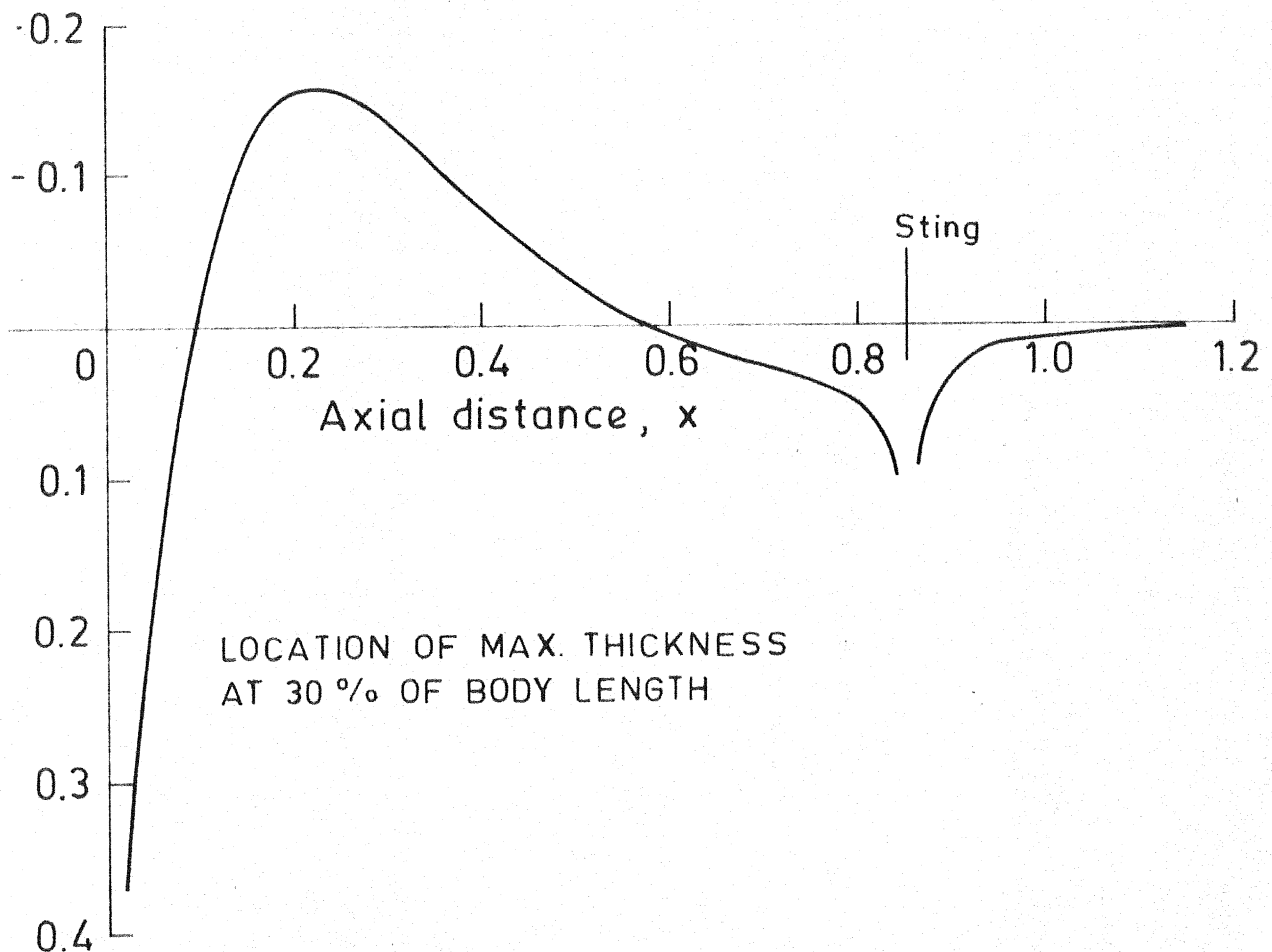
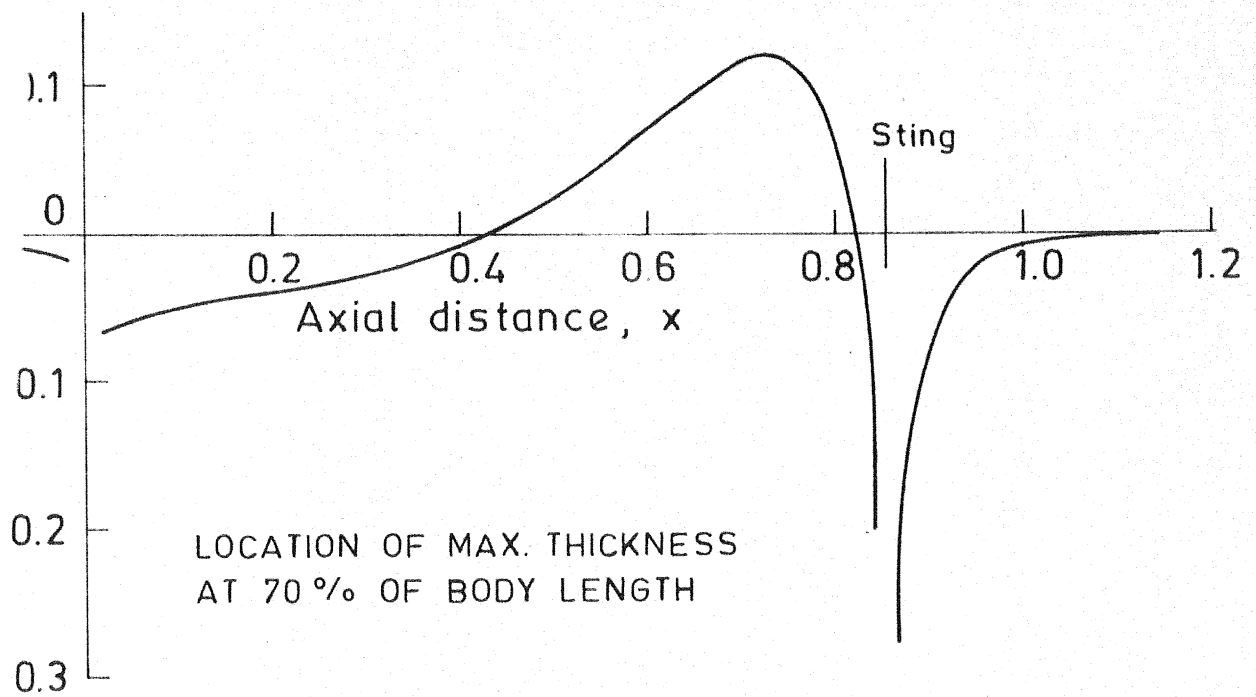
FIG. 9 DISTRIBUTION OF C_p ON PARABOLIC ARC OF REVOLUTION ($M_\infty = 0.9$, $FR = 10$, solid wall at 1.17).



10 DISTRIBUTION OF C_p ON PARABOLIC ARC OF REVOLUTION ($M_\infty = 0.90$, $FR = 10$, wall at 1.17).



1 DISTRIBUTION OF C_p ON PARABOLIC ARC OF REVOLUTION IN FREE AIR AT SUPER-CRITICAL SHOCK FREE MACH NUMBERS ($FR = 10$).



12 DISTRIBUTION OF C_p ON GENERAL PARABOLIC BODY OF REVOLUTION IN FREE AIR ($M_\infty = 0.9$, $FR = 10$).

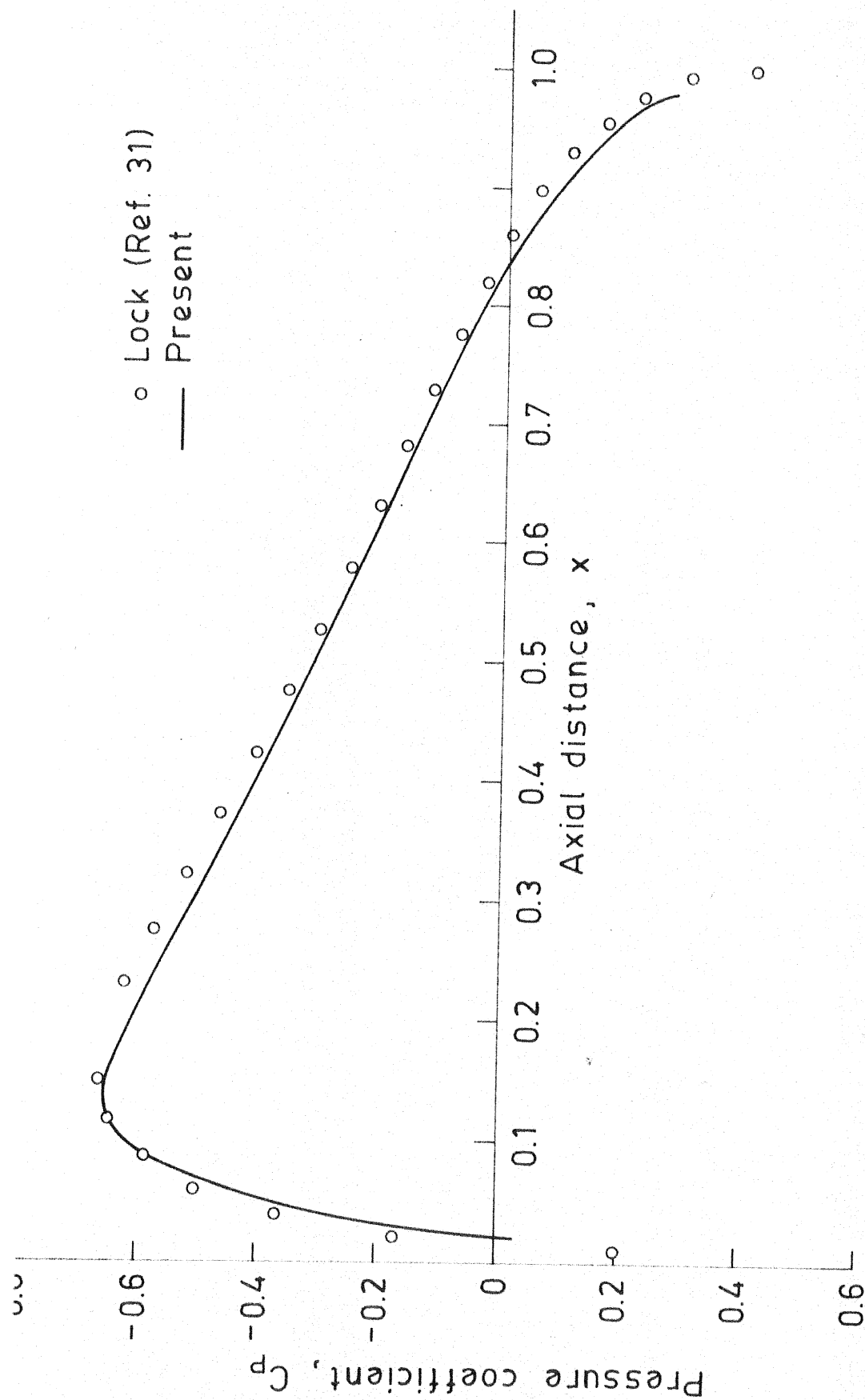


FIG. 13 DISTRIBUTION OF C_p ON NACA - 0012 AIR FOIL AT ZERO INCIDENCE IN FREE AIR ($M_\infty = 0.72$).

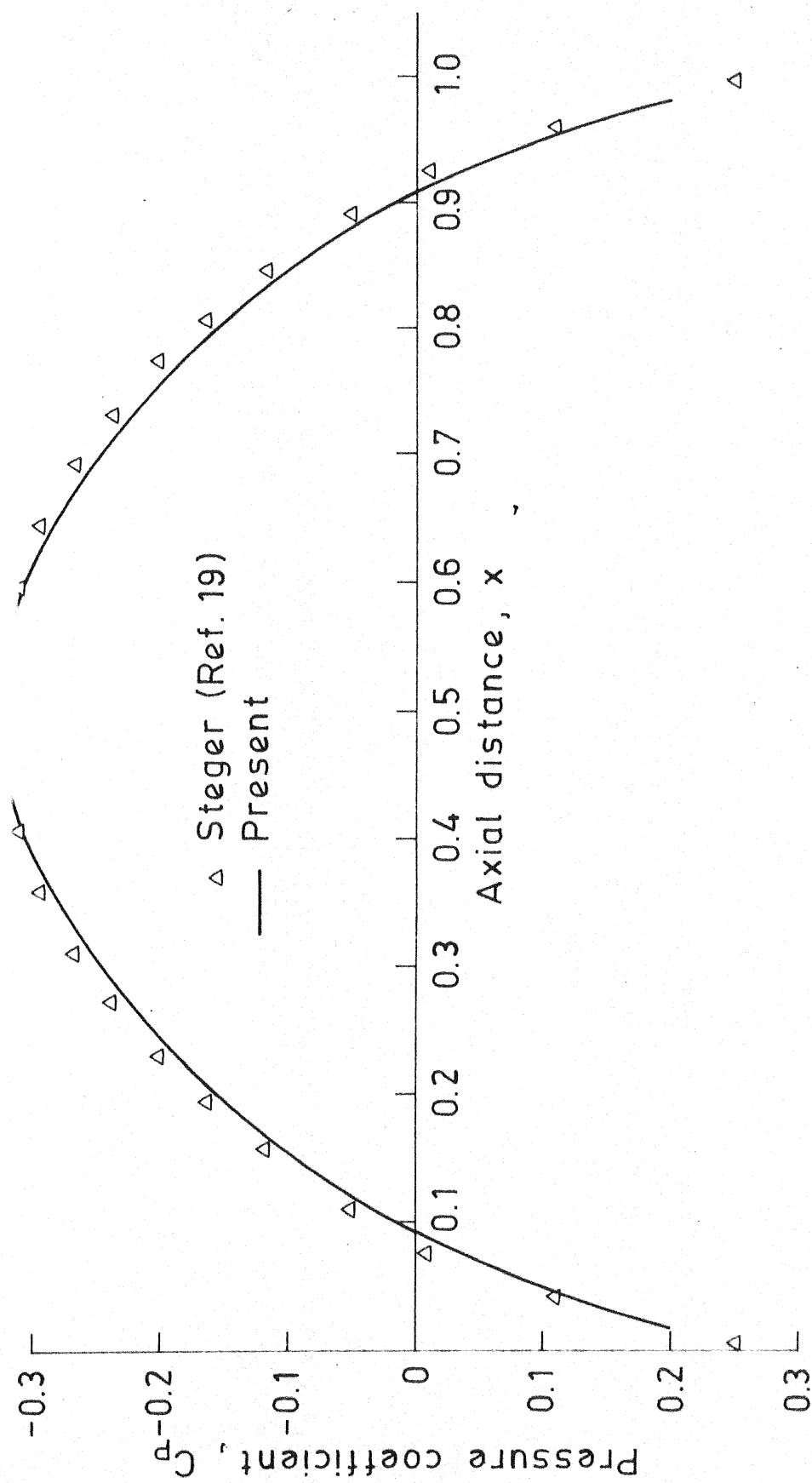


FIG. 14 DISTRIBUTION OF C_p ON 6% THICK PARABOLIC AIR
FOIL AT ZERO INCIDENCE ($M_\infty = 0.825$).

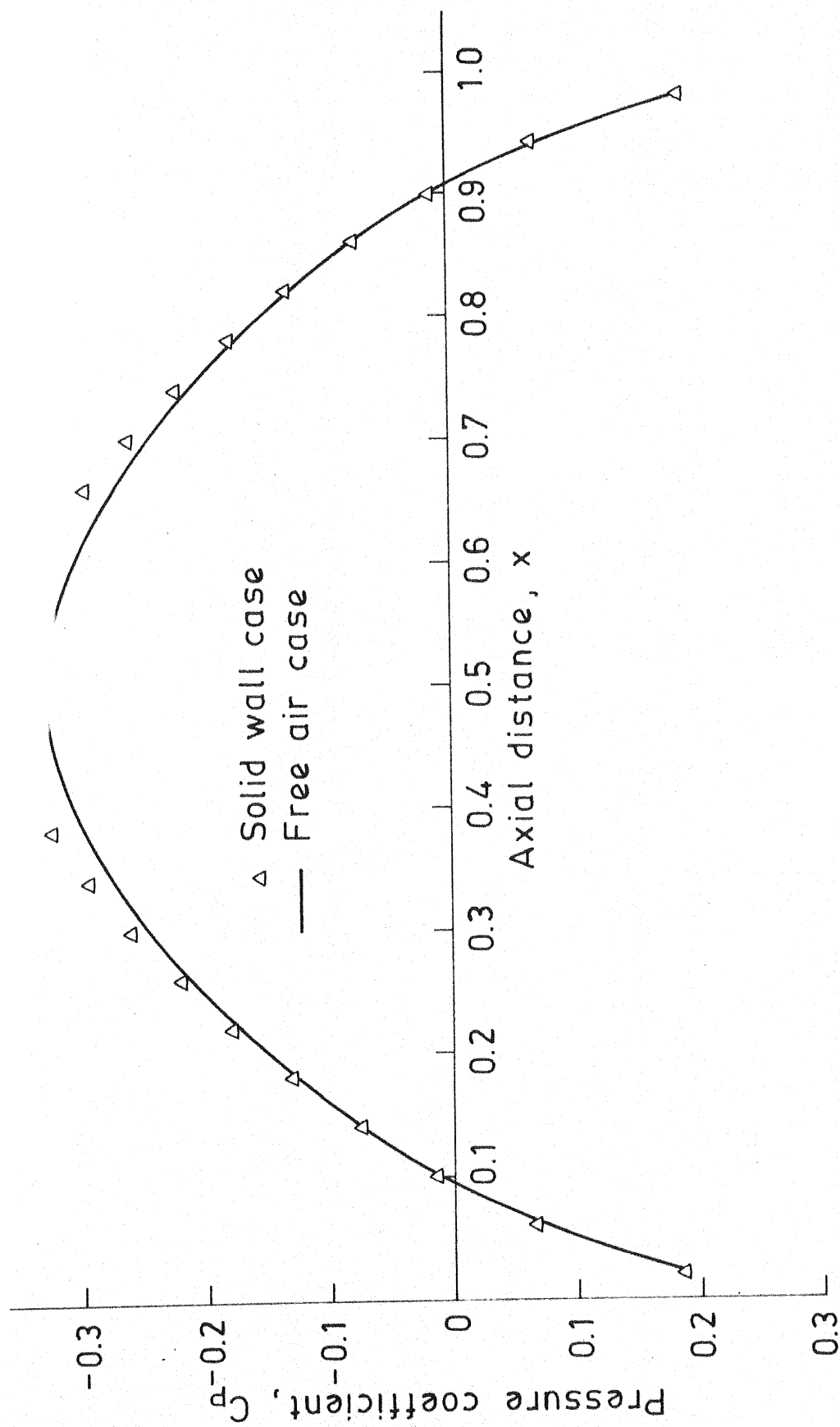


FIG. 15 DISTRIBUTION OF C_p ON 6% THICK PARABOLIC AIR FOIL AT ZERO INCIDENCE WITH WALL INTERFERENCE ($M_\infty = 0.825$, $h/c = 2.0$).

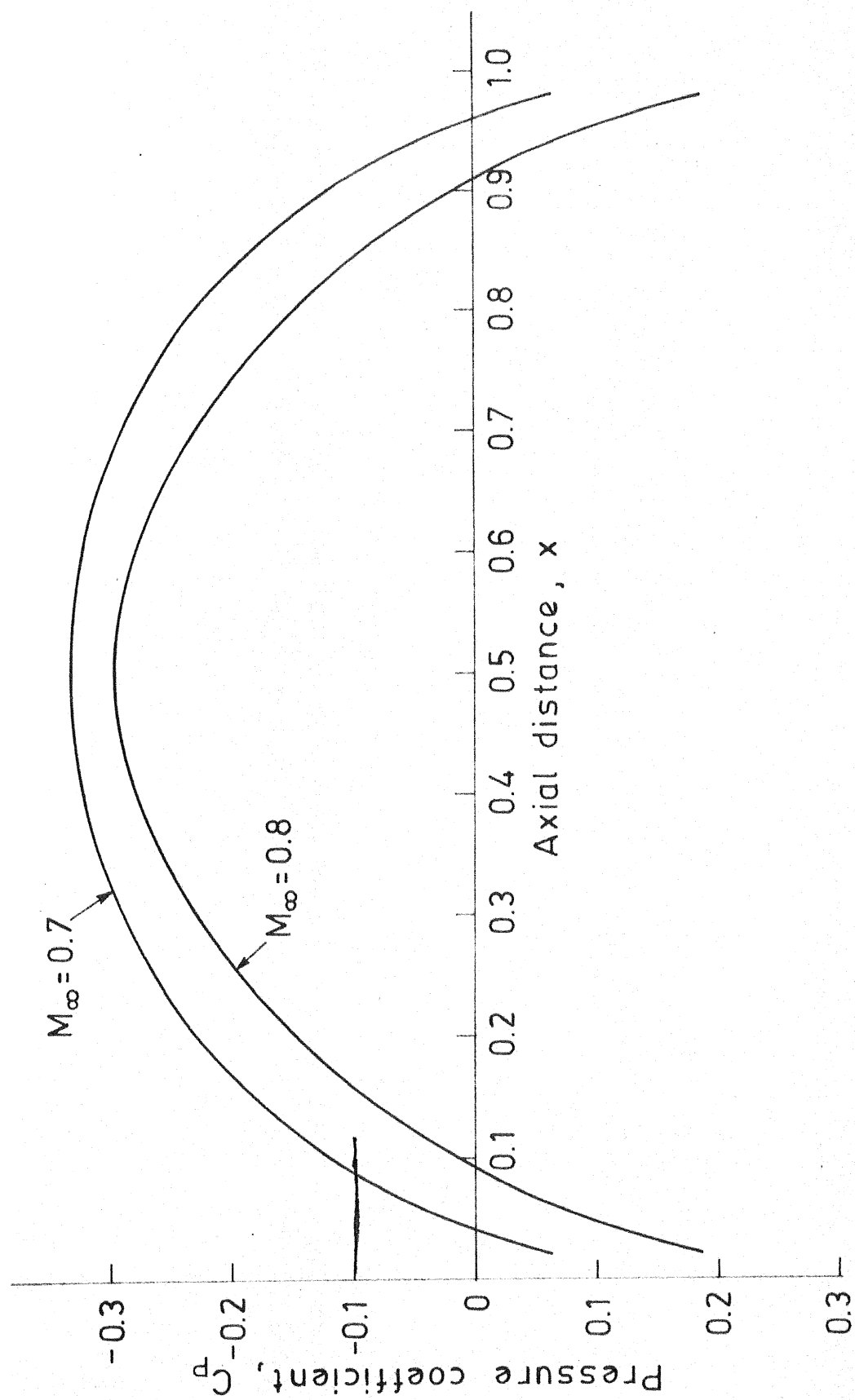


FIG. 16 DISTRIBUTION OF C_p ON 6% THICK PARABOLIC AIR FOIL AT ZERO INCIDENCE AT MACH NUMBERS 0.7 AND 0.8 IN FREE AIR BY PRESENT METHOD.

APPENDIX F

THIS PROGRAM CALCULATES PRESSURE DISTRIBUTION OVER A GENERAL
PARABOLIC BODY OF REVOLUTION IN FREE AIR OR IN POROUS WALL
WIND-TUNNEL

INPUT VARIABLES ARE:-
NB=NOS. OF POINTS TAKEN ON FULL LENGTH BODY
NR=NOS. OF INTERVALS TAKEN IN RADIAL DIRECTION
LP=FORE AND AFT EXTENT TAKEN IN PERCENT OF BODY LENGTH
MAX=MAXIMUM NOS. OF ITERATIONS ALLOWED
IS=0, FOR NO STING
1, WITH STING
XST=LOCATION OF STING
RS=RADIUS OF STING
IL=0, FOR FREE AIR CASE
1, FOR WALL INTERFERENCE CASE
FR=FINENESS RATIO OF THE BODY
M=FREE STREAM MACH NO
IEQ=EQUATION NO. USED (APPENDIX E)
CO, PO ARE CONSTANTS FOR THE BODY USED
RW=RADIUS OF WIND TUNNEL WALL
WP=POROSITY PARAMETER OF WALL

THIS IS MAIN PROGRAM

REAL M

INTEGER S, P

COMMON/INT/S, P, X(51), R(10), H(10), NX, NR, F(50,10), RB(50), AB(50,10)

COMMON/SE1/ DE, DY1, DY2, IST, NP

COMMON/SET1/DELX, IB, BB, IS

COMMON/SET2/RMAX, Y, RS

COMMON/EF/E, FE

COMMON/IW/AW(40,40,10), U1(40,10), WP, RW

COMMON/BDS/CO, PO, IEQ

DIMENSION ULL(50,10), UL(50,10), UNL(50,10), U(50,10)

1, AIN(50,10), E(101), FE(101), DB(40), CPL(40), CPNL(40)

TYPE 950

FORMAT(10X, 'TYPE NB NR LP MAX IS XST RS IL FR M IEQ CO PO')

ACCEPT *, NB, NR, LP, MAX, IS, XST, RS, IL, FR, M, IEQ, CO, PO

```

IF(IL.NE.0) TYPE 951
951  FORMAT(10X,"TYPE RW WP" )
      IF(IL.NE.0) ACCEPT *,RW,WP
      PRINT 810,NB,NR,LP,MAX
      PRINT 820,IS,XST,RS
      PRINT 830,IL,FR,M
      PRINT 831,IEQ,CO,PO
      IF(IL.NE.0) PRINT 840,RW,WP
840  FORMAT(6X,"RW=",F5.3,3X,"WP=",F5.3)
810  FORMAT(/6X,"NB=",I2,6X,"NR=",I2,6X,"LP=",I2,3X,"MAX=",I2)
820  FORMAT(6X,"IS=",I1,6X,"XST=",F5.3,3X,"RS=",F7.5)
830  FORMAT(6X,"IL=",I1,7X,"FR=",F5.2,4X,"M=",F5.3)
831  FORMAT(5X,"IEQ=",I1,7X,"CO=",F6.3,2X,"PO=",F6.3)
      IF(IS.NE.0) PRINT 910
      IF(IL.EQ.0) PRINT 920
      IF(IL.NE.0) PRINT 930
910  FORMAT(/10X,"BODY WITH STING")
920  FORMAT(/10X,"FREE AIR CASE")
930  FORMAT(/10X,"WALL INTERFERENCE CASE")
      ERROR=0.001
      Y=XST
      RMAX=0.5/FR
      G=1.4
91  FORMAT(10X,F7.3,12F9.4)
      DELX=1./FLOAT(NB)
      BB=1.-M*M
      CONS=(G+1.) *M*M/BB
      NP=NB*LP/100
      X(1)=(0.5-FLOAT(NP))*DELX
      IB=NB
      IF(IS.NE.0) IB=Y*FLOAT(NB)+0.51
      NX=IB+2*NP
      IF(IS.GT.0) NX=NX+2
      IST=IB+NP
      X(IST)=0.0
      DO 10 I=2,NX
      IF(IS.EQ.1) X(IST+1)=X(IST)
      X(I)=X(I-1)+DELX
10  CONTINUE
      X(NX+1)=X(NX)+DELX
      IF(IS.EQ.0) GO TO 11
      ST=X(IST)+0.5*DELX
      DE=Y-ST
      DY1=(DELX+DE)/2.
      DY2=DELX-DE
      X(IST)=X(IST-1)+0.5*(DELX+DY1)
      X(IST+1)=X(IST)+DY1
      X(IST+2)=X(IST+1)+0.5*(DY1+DY2)

```



```

11 IF(NP.EQ.0) NX=NX-1
CONTINUE
H(1)=RMAX
R(1)=H(1)
DO 20 J=2,NR
H(J)=2.*RMAX
R(J)=R(J-1)+H(J-1)+H(J)
20 CONTINUE
IF(IL.NE.0) H(NR)=(RW-(R(NR-1)+H(NR-1)))*0.5
IF(IL.NE.0) R(NR)=R(NR-1)+H(NR-1)+H(NR)
DO 31 I=1,NX
XI=X(I)
CALL SURF(XI,RJ,DR1,0.0)
RB(1)=RJ
DB(1)=DR1
UL1=UB(XI)
OBL(1,1)=UL1
OB(1,1)=UL1*CONS
O1(1,1)=OB(1,1)
F(1,1)=O1(1,1)*O1(1,1)
DO 30 J=2,NR
RJ=R(J)
CALL LINEAR(XI,RJ,UL1,CPL)
OBL(1,J)=UL1
OB(1,J)=UL1*CONS
O1(1,J)=OB(1,J)
F(1,J)=O1(1,J)*O1(1,J)
30 CONTINUE
31 CONTINUE
AIWL=0.0
AINTG=0.0
DO 60 IT=1,MAX
DO 41 S=1,NX
DO 42 P=1,NR
CALL INTEG(AINTG)
IF((IL.NE.0).AND.(IT.EQ.1)) CALL WALL
IF(IL.NE.0) CALL INTWA(AIWL)
ANU2=-AB(S,P)/3.141592654
U(S,P)=(UB(S,P)-AINTG-ANU2*F(S,P)+AIWL)/(1.-ANU2*O1(S,P))
AIN(S,P)=AINTG-AIWL
42 CONTINUE
41 CONTINUE
DO 51 I=1,NX
DO 50 J=1,NR
IF(ABS(O(1,J)-O1(1,J)).GT.ERROR) GO TO 100
50 CONTINUE
51 CONTINUE
PRINT 92,IT

```

```

92     FORMAT(10X,12,'TH ITERATION')
      DO 52 I=1,NX
      DO 53 J=1,NR
      UBL(I,J)=U(I,J)/CONS
53     CONTINUE
      DRR=0.0
      DR1=DRB(1)
      DRR=DR1*DR1
      CPL(I)=-2.*UBL(I,1)-DRR
      CPNL(I)=-2.*UNL(I,1)-DRR
52     CONTINUE
      PRINT 93,(R(J),J=2,NR)
93     FORMAT(/22X,'R=BODY SURF',8X,'R=',F6.3,10X,'R=',F6.3,10X,
      1'R=',F6.3,10X,'R=',F6.3,10X,'R=',F6.3/14X,'X',7X,'UL',6X,
      2'UNL',7X,'UL',6X,'UNL',7X,'UL',6X,'UNL')
      PRINT 91,(X(1),(UBL(I,J),UNL(I,J),J=1,NR),I=1,NX)
      PRINT 94
94     FORMAT(/10X,'COEFF. OF PRESS. DIST. ON BODY SURFACE'/14X,'X',
      18X,'CP-LINEAR',6X,'CP-NON LINEAR',4X,'RED. PERT. VEL. U')
      PRINT 95,(X(1),CPL(I),CPNL(I),U(I,1)),I=1,NX)
95     FORMAT(10X,F7.3,5X,F9.4,9X,F9.4,7X,F9.4)
      STOP
100    DO 62 I=1,NX
      DO 61 J=1,NR
      U1(I,J)=U(I,J)
      F(I,J)=U1(I,J)*U1(I,J)
61     CONTINUE
62     CONTINUE
60     CONTINUE
      STOP
      END

C
C
C *****
C THIS SUBROUTINE CALCULATES THE BODY RADIUS AND ITS DERIVATIVES
C AT DESIRED LOCATIONS
C SUBROUTINE SURF(X,R,DR,DDR)
C   COMMON/SET2/RMAX,Y,RS
C   COMMON/BDS/C,P,IEQ
C   ZER=0.0
C   R=ZER
C   DR=ZER
C   DDR=ZER
C   IF(X,LT,ZER)RETURN
C   R=RS
C   IF(X,GT,Y) RETURN
C   CR=C*RMAX
C   B=X

```

```

IF(LEQ, EQ, 1) B=1.-X
AB=0.0
IF(B.LT.0.0001) GO TO 111
AB=B** (P-1.)
R=CR*B*(1.-AB)
DDR=-CR*P*(P-1.)*AB/B
111 DR=CR*(1.-P*AB)*(-1.)*1EQ
RETURN
END

```

```

C
C
C *****
C THIS FUNCTION CALCULATES DERIVATIVE OF BODY CROSS-SECTIONAL
C AREA AT AXIAL LOCATION X
C FUNCTION DS(X)
C CALL SURF(X,R,DR,DDR)
C DS=R/2.*DR
C RETURN
C END

```

```

C
C
C *****
C THIS FUNCTION CALCULATES SECOND DERIVATIVE OF BODY CROSS-
C SECTIONAL AREA AT X
C FUNCTION DDS(X)
C CALL SURF(X,R,DR,DDR)
C DDS=0.5*(DR*DR+R*DDR)
C RETURN
C END

```

```

C
C
C *****
C THIS IS AUXILIARY FUNCTION IN CALCULATING UB(X)
C FUNCTION FCT(X,E)
C FCT=0.0
C DIF=ABS(X-E)
C IF(DIF.LT.0.0001) RETURN
C F=DDS(X)-DDS(E)
C FCT=F/DIF
C RETURN
C END

```

```

C
C
C *****
C THIS FUNCTION CALCULATES LINEAR PERTURBATION VELOCITY OVER
C BODY SURFACE AT AXIAL LOCATION X
C FUNCTION UB(X)
C COMMON/SET1/DELX, LB, BB, IS

```

```

COMMON/SET2/RMAX,Y,RS
DEL=DEIX
SUM=0.0
E3=0.0
DO 10 I=1,IB
E1=E3
E2=E1+0.5*DEL
E3=E1+DEL
SIMP=FCT(X,E1)+FCT(X,E2)*4.0+FCT(X,E3)
SUM=SUM+SIMP
10 CONTINUE
SUM=DEL/6.*SUM
IF(IS.EQ.0) GO TO 100
SUM=SUM+(Y-E3)/2.*(FCT(X,Y)+FCT(X,E3))
100 CONTINUE
SLEF=DS(Y)/ABS(X-Y)
CALL SURF(X,R,DR,DOR)
IF(X.GT.0.0.AND.X.GT.Y) SLEF=SLEF+DOS(X)*ALOG(BB*R*R/(4.*X*(Y-X)))
OB=SUM+SLEF
RETURN
END

```

```

C
C
C *****
C THIS SUBROUTINE CALCULATES LINEAR PERTURBATION VELOCITY
C AWAY FROM BODY SURFACE
C SUBROUTINE LINEAR(X,R,UL,CPL)
COMMON/SET1/DEIX,IB,BB,IS
COMMON/SE1/ DE,DY1,DY2, IST,NP
DEL=DEIX/2.
I2=2*IB
BR=BB*R*R
E=-0.5*DEL
SUM=0.0
DO 400 J=1,I2
E=E+DEL
D=X-E-0.5*DEL
PP=1./SQRT(D*D+BR)
QQ=1./SQRT((D+DEL)*(D+DEL)+BR)
SUM=SUM+DS(E)*(PP-QQ)
400 CONTINUE
IF(IS.NE.1) GO TO 100
E=E+0.5*(DEL+DE)
D=X-E-0.5*DE
SUM=SUM+DS(E)*(1./SQRT(D*D+BR)-1./SQRT((D+DE)**2+BR))
100 CONTINUE
UL=SUM
CPL=-2.*UL

```

RETURN
END

```

*****
THIS SUBROUTINE EVALUATES THE FIELD INTEGRAL
SUBROUTINE INTEG(AINTG)
INTEGER S,P
REAL KK
COMMON/INT/S,P,X(51),R(10),H(10),NX,NR,F(50,10),RB(50),AB(50,10)
COMMON/SEL/ DE,DY1,DY2, IST,NP
COMMON/SET1/DETX,IB,BB,IS
COMMON/EF/E,FE
DIMENSION A(51,10),BR(10),BH(10),E(101),FE(101)
NX1=NX+1
B=SQRT(BB)
BRP=B*R(P)
IF(P.EQ.1) BRP=B*RB(S)
DO 9 J=1,NR
BH(J)=B*H(J)
BR(J)=B*R(J)
CONTINUE
SUM=0.0
DO 10 I=1,NX1
DELT=DETX
IF(IS.NE.1) GO TO 8
IF(I.EQ.1ST.OR,I.EQ.(1ST+1)) DELT=DY1
IF(I.EQ.(1ST+2)) DELT=DY2
CONTINUE
XSI=X(S)-X(1)+0.5*DELT
IF(I.EQ.1) GO TO 20
BRI=B*RB(I-1)
RPL=BRI+BRP
RRP=RPL*RPL
XR=SQRT(XSI*XSI+RRP)
XRM=SQRT(XSM*XSM+RRP)
AK=4.0*BRP*BRI
KK=AK/(XR*XR)
CALL INTPOL(KK,E,EK)
KK=AK/(XRM*XRM)
CALL INTPOL(KK,E,EKM)
RMN=BRI-BRP
BHR=2.0*BH(1)-BRI
RRN=RMN*(BHR+RMN)
AIB=BRI*(EK/XR*ATAN(BHR*XSI/(XSI*XSI+RRN))-EKM/XRM*ATAN(BHR*XSM
1/(XSM*XSM+RRN)))
AB(I-1,1)=AIB
SUM=SUM+F(I-1,1)*AB(I-1,1)

```

```

20  CONTINUE
    XSM=XSI
    DO 21 J=2,NR
        RPLUS=BR(J)+BRP
        XR=SQRT(XSI*XSI+RPLUS*RPLUS)
        KK=4.0*BRP*BR(J)/(XR*XR)
        CALL INTPOL(KK,E,EK)
        RMNS=BR(J)-BRP
        A(I,J)=BR(J)/XR*EK*(ATAN((RMNS+BH(J))/XSI)-ATAN((RMNS-BH(J))/XSI))
        IF(I.EQ.1) GO TO 21
        AB(I-1,J)=A(I,J)-A(I-1,J)
        SUM=SUM+F(I-1,J)*AB(I-1,J)
21  CONTINUE
10  CONTINUE
    AINTG=.5/3.141592654*SUM
    RETURN
    END

```

```

C
C
C *****
C THIS SUBROUTINE INTERPOLATES LINEARLY A FUNCTION BETWEEN TWO
C POINTS
C SUBROUTINE INTPOL(AK,FCT,VAL)
C DIMENSION FCT(101)
C CKK=100.*AK
C M=CKK+1.0
C DIF=CKK-FLOAT(M)
C VAL=FCT(M)+(FCT(M+1)-FCT(M))*DIF
C RETURN
C END

```

```

C
C
C *****
C THIS SUBROUTINE EVALUATES COEFFICIENTS FOR WALL INTEGRAL
C SUBROUTINE WALL
C INTEGER S,P
C REAL KK,K1,KI1
C COMMON/IW/AW(40,40,10),U1(40,10),WP,RW
C COMMON/SET1/DELX,IB,BB,IS
C COMMON/SE1/ DE,DY1,DY2, IST,NP
C COMMON/EF/E,FE
C COMMON/INT/S,P,X(51),R(10),H(10),NX,NR,F(50,10),RB(50),AB(50,10)
C DIMENSION E(101),FE(101)
C B=SQRT(BB)
C BRW=B*RW
C BRP=B*R(P)
C IF(P.EQ.1)BRP=B*RB(S)
C BPL=BRW+BRP

```

```

XSI=X(S)-X(1)+0.5*DELT
YI=SQRT(XSI*XSI+BPL*BPL)
IF(BRP,LT,0.0001) GO TO 12
BSQ=SQRT(BRW*BRP)
BMN=BRW-BRP
BRPI=BRW/4./3.141592654
KI=2.*BSQ/YI
TI=ATAN(-XSI*KI/BMN)
ALI=ALOG(-XSI+YI)
CLI=ALOG((1.-KI)/(1.+KI))
DO 10 I=1,NX
  I1=I+1
  DELT=DELT
  IF(1S.NE.1) GO TO 8
  IF(I1.EQ.1ST,OR,I1.EQ.(1ST+1)) DELT=DY1
  IF(I1.EQ.(1ST+2)) DELT=DY2
  CONTINUE
  XSI1=X(S)-X(I1)+0.5*DELT
  YI1=SQRT(XSI1*XSI1+BPL*BPL)
  KI1=2.*BSQ/YI1
  TI1=ATAN(-XSI1*KI1/BMN)
  ALI1=ALOG(-XSI1+YI1)
  CLI1=ALOG((1.-KI1)/(1.+KI1))
  KK=4.*BRW*BRP/((X(S)-X(I1))**2+BPL*BPL)
  CALL INTPOL(KK,E,EI)
  CALL INTPOL(KK,FI,FI)
  IF((KK=.9900).GT,0.000001) FI=0.5*ALOG(16.0/(1.-KK))
  AW(1,S,P)=(EI/BSQ*(2.*(TI1-TI)-WP/B*(CLI1-CLI))+2.0/BRW*(FI-EI)
  1*(ALI1-ALI))*BRPI
  XSI=XSI1
  YI=YI1
  KI=KI1
  TI=TI1
  CLI=CLI1
  ALI=ALI1
  CONTINUE
  GO TO 21
10 CONTINUE
12 DO 20 I=1,NX
  I1=I+1
  DELT=DELT
  IF(1S.NE.1) GO TO 7
  IF(I1.EQ.1ST,OR,I1.EQ.(1ST+1)) DELT=DY1
  IF(I1.EQ.(1ST+2)) DELT=DY2
  CONTINUE
  XSI1=X(S)-X(I1)+0.5*DELT
  YI1=SQRT(XSI1*XSI1+BRW*BRW)
  AW(1,S,P)=0.5*(BRW/B*WP*(1./YI1-1./YI)-XSI1/YI1+XSI/YI)

```

```

XSI=XSI1
YI=YI1
CONTINUE
CONTINUE
RETURN
END

```

```

*****
THIS SUBROUTINE CALCULATES THE WALL INTEGRAL
SUBROUTINE INTWA(AIWL)
INTEGER S,P
COMMON/INT/S,P,X(51),R(10),H(10),NX,NR,F(50,10),RB(50),AB(50,10)
COMMON/IW/AW(40,40,10),UI(40,10),WP,RW
SUM=0.0
DO 10 I=1,NX
SUM=SUM+UI(I,NR)*AW(I,S,P)
CONTINUE
AIWL=SUM
RETURN
END

```

```

*****
FOLLOWING ARE THE VALUES OF COMPLETE ELLIPTICAL INTEGRALS OF
SECOND AND FIRST KINDS
BLOCK DATA
DIMENSION E(101),FE(101)
COMMON/EF/E,FE
DATA E/1.570796,1.566862,1.562913,1.558948,1.554969,1.550973,
11.546962,1.542936,1.538893,1.534833,1.530758,1.526665,1.522555,
21.518428,1.514284,1.510122,1.505942,1.501743,1.497526,1.493290,
31.489035,1.484761,1.480466,1.476152,1.471817,1.467462,1.463086,
41.458688,1.454269,1.449827,1.445363,1.440876,1.436366,1.431832,
51.427274,1.422691,1.418083,1.413450,1.408791,1.404105,1.399392,
61.394652,1.389883,1.385086,1.380259,1.375402,1.370515,1.365596,
71.360645,1.355661,1.350644,1.345592,1.340505,1.335382,1.330222,
81.325024,1.319788,1.314511,1.309192,1.303832,1.298428,1.292979,
91.287484,1.281942,1.276350,1.270707,1.265013,1.259263,1.253458,
11.247595,1.241671,1.235684,1.229632,1.223512,1.217321,1.211056,
21.204714,1.198290,1.191781,1.185183,1.178490,1.171697,1.164798,
31.157787,1.150656,1.143396,1.135998,1.128451,1.120741,1.112856,
41.104775,1.096478,1.087937,1.079121,1.069986,1.060474,1.050502,
51.039947,1.028595,1.015994,1.000000/,
1FE/1.570796,1.574746,1.578740,1.582780,1.586868,1.591003,
21.595188,1.599423,1.603710,1.608049,1.612441,1.616889,1.621393,
31.625955,1.630575,1.635257,1.640000,1.644806,1.649678,1.654617,
41.659624,1.664701,1.669850,1.675073,1.680373,1.685750,1.691208,

```


51.696749,1.702374,1.708087,1.713889,1.719785,1.725776,1.731865,
61.738055,1.744351,1.750754,1.757268,1.763898,1.770647,1.777520,
71.784519,1.791650,1.798918,1.806328,1.813884,1.821593,1.829460,
81.837491,1.845694,1.854075,1.862641,1.871400,1.880361,1.889533,
91.898925,1.908547,1.918410,1.928526,1.938908,1.949568,1.960521,
11.971783,1.983371,1.995303,2.007598,2.020279,2.033369,2.046894,
22.060882,2.075363,2.090373,2.105948,2.122132,2.138970,2.156516,
32.174827,2.193970,2.214022,2.235068,2.257205,2.280549,2.305232,
42.331409,2.359264,2.389016,2.420933,2.455338,2.492635,2.533335,
52.578092,2.627773,2.683551,2.747073,2.820752,2.908337,3.016112,
63.155875,3.354141,3.695367,999999.9/
END

THIS PROGRAM CALCULATES PRESSURE DISTRIBUTION OVER A PARABOLIC
ARC AIRFOIL IN FREE AIR OR IN POROUS WALL WIND TUNNEL

INPUT VARIABLES:-
NB=NOS. OF POINTS TAKEN ON AIRFOIL CHORD LENGTH
NR=NOS. OF POINTS TAKEN IN LATERAL DIRECTION
LP=FORE AND AFT EXTENT TAKEN IN % OF AIRFOIL LENGTH
MAX=MAXIMUM NOS. OF ITERATIONS ALLOWED
T=THICKNESS RATIO OF AIRFOIL
M=FREE STREAM MACH NO.
IL=0, FOR FREE AIR CASE
1, FOR WALL INTERFERENCE CASE
YW=HALF HEIGHT OF THE WIND TUNNEL
WP=POROSITY PARAMETER OF WALL

THIS IS THE MAIN PROGRAM

REAL M

INTEGER S,P

COMMON/U1/S,P,NX,NR

COMMON/U2/U1(40,10),W(40,40,10)

COMMON/U3/X(40),Y(10),H(10),WP,B,DELX,YW

COMMON/U4/F(40,10),A(40,10),YBPL(40),YBMN(40)

COMMON/TY/T

COMMON/U5/ULL(40,10),UNL(40,10),M,G

DIMENSION U(40,10),UB(40,10),AA(10)

FORMAT(10X,F7.3,12F9.4)

ERROR=0.001

TYPE 950

FORMAT(10X,'TYPE NB,NR,LP,MAX,T,M,IL')

ACCEPT *,NB,NR,LP,MAX,T,M,IL

IF(IL.NE.0) TYPE 951

FORMAT(10X,'TYPE YW,WP')

IF(IL.NE.0) ACCEPT *,YW,WP

PRINT 810,NB,NR,LP,MAX

PRINT 820,IL,T,M

IF(IL.NE.0) PRINT 830,YW,WP

FORMAT(76X,'NB=',I2,6X,'NR=',I2,6X,'LP=',I2,3X,'MAX=',I2)

FORMAT(6X,'IL=',I1,8X,'T=',F5.3,4X,'M=',F5.3)

FORMAT(6X,'YW=',F5.3,3X,'WP=',F5.3)

IF(IL.EQ.0) PRINT 910

IF(IL.NE.0) PRINT 920

FORMAT(710X,'FREE AIR CASE')

```

920      FORMAT(/10X,'WALL INTERFERENCE CASE')
      NY=NR
      NR1=1
      NR2=2
      YMAX=T/2.
      G=1.4
      DELX=1./FLOAT(NB)
      B=SQRT(1.-M*M)
      CONS=(G+1.)*M*M/(B*B)
      NP=NB*LP/100
      X(1)=(0.5-FLOAT(NP))*DELX
      NX=NB+2*NP
      DO 10 I=2,NX
10      X(I)=X(I-1)+DELX
      CONTINUE
      IF(LH,NE,0) GO TO 11
      Y(1)=YMAX
      Y(2)=7.*YMAX
      H(1)=Y(1)
      H(2)=5.*YMAX
      DO 20 J=3,NR
      H(J)=H(J-1)+5.*YMAX
      Y(J)=Y(J-1)+H(J-1)+H(J)
20      CONTINUE
      GO TO 22
11      DH=0.5*YW/(NR-1)
      H(1)=DH/2.
      Y(1)=H(1)
      H(2)=DH
      Y(2)=2.*DH
      DO 21 J=3,NR
      H(J)=H(J-1)
      Y(J)=Y(J-1)+H(J-1)+H(J)
21      CONTINUE
      H(NR)=H(1)
      Y(NR)=Y(NR-1)+H(NR-1)+H(NR)
22      CONTINUE
      DO 31 I=1,NX
      X1=X(I)
      YBPL(1)=YY(X1)
      YJ=0.000001
      UB(1,1)=CONS*UL(X1,YJ)
      F(1,1)=UB(1,1)*UB(1,1)
      Uf(1,1)=UB(1,1)
      DO 30 J=2,NR
      YJ=Y(J)*B
      UB(1,J)=CONS*UL(X1,YJ)
      F(1,J)=UB(1,J)*UB(1,J)

```

```

30      U1(I,J)=UB(I,J)
31      CONTINUE
      Y(1)=0.0
      AIWL=0.0
      DO 40 IT=1,MAX
      DO 41 S=1,NX
      DO 42 P=1,NY
          CALL INTEG(AINTG)
          IF(IT.EQ.1,AND(IL.NE.0) CALL WALL
          IF(IL.NE.0) CALL INTWA(AIWL)
          AA(P)=AINTG+AIWL
          ANU2=A(S,P)
          U(S,P)=(UB(S,P)+AINTG-ANU2*F(S,P)+AIWL)/(1.-ANU2*U1(S,P))
42      CONTINUE
41      CONTINUE
      DO 51 I=1,NX
      DO 50 J=1,NY
          IF(ABS(U(I,J)-U1(I,J)).GT.ERROR) GO TO 100
50      CONTINUE
51      CONTINUE
      PRINT 92,IT
92      FORMAT(10X,I2,'TH ITERATION')
      PRINT 93,(Y(J),J=1,NR)
93      FORMAT(/23X,'Y=',F6.3,10X,'Y=',F6.3,10X,'Y=',F6.3,10X,
          1*'Y=',F6.3,10X,'Y=',F6.3,10X,'Y=',F6.3/14X,'X',7X,'UL',
          26X,'UNL',7X,'UL',6X,'UNL',7X,'UL',6X,'UNL',7X,'UL',
          36X,'UNL',7X,'UL',6X,'UNL',7X,'UL',6X,'UNL')
      DO 52 I=1,NX
      DO 53 J=1,NY
          UNL(I,J)=U(I,J)/CONS
          ULL(I,J)=UB(I,J)/CONS
53      CONTINUE
      PRINT 91,X(I),( ULL(I,J),UNL(I,J) ,J=1,NR)
52      CONTINUE
      CALL OUTPUT
      STOP
100     DO 62 I=1,NX
          DO 61 J=1,NY
              U1(I,J)=U(I,J)
              F(I,J)=U(I,J)*U(I,J)
61      CONTINUE
62      CONTINUE
60      CONTINUE
      STOP
      END

```

C

C

```

C *****
C THIS SUBROUTINE CALCULATES FIELD INTEGRAL
SUBROUTINE INTEG(AINTG)
  INTEGER S,P
  COMMON/U1/S,P,NX,NR
  COMMON/U3/X(40),Y(10),H(10),WP,B,DELX,YW
  COMMON/U4/F(40,10),A(40,10),YBPL(40),YBMN(40)
  NY=NR
  SUM=0.0
  C=1./4./3.141592654
  X1=X(S)-X(1)+0.5*DELX
  DO 10 I=1,NX
    X2=X1-DELX
    Y1=Y(P)*B
    Y2=(Y(P)-2.*H(1))*B
    Y3=Y(P)*B
    Y4=(Y(P)+2.*H(1))*B
    AI1=ATAN(Y1/X2)-ATAN(Y1/X1)-ATAN(Y3/X2)+ATAN(Y3/X1)
    AI2=-ATAN(Y2/X2)+ATAN(Y2/X1)+ATAN(Y4/X2)-ATAN(Y4/X1)
    A(I,1)=-C*(AI1+AI2)
    SUM=SUM+F(I,1)*A(I,1)
  DO 12 J=2,NY
    AI1=-AI2
    Y2=Y2-2.*H(J)*B
    Y4=Y4+2.*H(J)*B
    AI2=-ATAN(Y2/X2)+ATAN(Y2/X1)+ATAN(Y4/X2)-ATAN(Y4/X1)
    A(I,J)=-C*(AI1+AI2)
    SUM=SUM+F(I,J)*A(I,J)
12  CONTINUE
    X1=X2
10  CONTINUE
  AINTG=SUM
  RETURN
  END

```

```

C *****
C THIS SUBROUTINE EVALUATES COEFFICIENTS FOR WALL INTEGRAL
SUBROUTINE WALL
  INTEGER S,P
  COMMON/U1/S,P,NX,NR
  COMMON/U2/U1(40,10),W(40,40,10)
  COMMON/U3/X(40),Y(10),H(10),WP,B,DELX,YW
  COMMON/U4/F(40,10),A(40,10),YBPL(40),YBMN(40)
  NY=NR
  CW=-1./2./3.141592654
  Y1=B*(Y(P)-YW)
  Y2=B*(Y(P)+YW)

```

```

YY1=Y1*Y1
YY2=Y2*Y2
X1=X(S)-X(1)+0.5*DELX
XX1=X1*X1
A1=ALOG((XX1+YY1)*(XX1+YY2))
B1=ATAN(X1/Y1)-ATAN(X1/Y2)
DO 10 I=1,NX
X2=X1-DELX
XX2=X2*X2
A2=ALOG((XX2+YY1)*(XX2+YY2))
B2=ATAN(X2/Y1)-ATAN(X2/Y2)
DI=0.5*WP/B*(A2-A1)-(B2-B1)
W(I,S,P)=CW*DI
X1=X2
A1=A2
B1=B2
10 CONTINUE
RETURN
END

C
C
C *****
C THIS SUBROUTINE CALCULATES WALL INTEGRAL
C SUBROUTINE INTWA(AIWL)
C INTEGER S,P
C COMMON/D1/S,P,NX,NR
C COMMON/D2/U1(40,10),W(40,40,10)
C NY=NR
C SUM=0.0
C DO 10 I=1,NX
C SUM=SUM+U1(I,NY)*W(I,S,P)
10 CONTINUE
AIWL=SUM
RETURN
END

C
C
C *****
C THIS SUBROUTINE CALCULATES PRESSURE DISTRIBUTION
C SUBROUTINE OUTPUT
C REAL M
C COMMON/D0/ULL(40,10),UNL(40,10),M,G
C COMMON/D1/S,P,NX,NR
C COMMON/D3/X(40),Y(10),H(10),WP,B,DELX,YW
C CP(Q2)=A1*((1.+A2*(1.-Q2))**EX-1.)
92 FORMAT(10X,'MACH NO.='F7.3,10X,'PARABOLIC AIRFOIL')
93 FORMAT(8X,'X CP LIN CP PRESENT')
94 FORMAT(5X,F7.3,8F11.3)

```

```

PRINT 92,M
PRINT 93
SM=M*M
A1=2./G/SM
A2=(G-1.)*SM/2.
EX=G/(G-1.)
DO 10 I=1,NX
XI=X(I)
DYX=DY(XI)
QL=(1.+UJL(I,1))*2+DYX*DYX
QN=(1.+UNL(I,1))*2+DYX*DYX
CPL=CP(QL)
CPN=CP(QN)
PRINT 94,XI,CPL,CPN
10 CONTINUE
RETURN
END

```

```

*****
*****
THE FOLLOWING PACKAGE SHOULD BE REPLACED BY APPROPRIATE FUNCTIONS
IF THE BODY PROFILE IS CHANGED

```

```

*****
*****
THE FOLLOWING PACKAGE CALCULATES FUNCTIONS FOR BODY PROFILE
ITS DERIVATIVE AND LINEAR PERTURBATION VELOCITY FOR A PARABOLIC
AIRFOIL.

```

```

THIS FUNCTION CALCULATES AIRFOIL PROFILE
FUNCTION YY(X)
COMMON/TY/T
YY=0.0
IF(X.LT.0.0.OR.X.GT.1.0) RETURN
YY=2.0*T*X*(1.0-X)
RETURN
END

```

```

THIS FUNCTION CALCULATES THE DERIVATIVE OF AIRFOIL PROFILE
FUNCTION DY(X)
COMMON/TY/T
DY=0.0
IF(X.LT.0.0.OR.X.GT.1.0) RETURN

```

```
DY=2.0*T*(1.0-2.*X)
RETURN
END
```

C
C
C

```
THIS FUNCTION CALCULATES LINEAR PERTURBATION VELOCITY
FUNCTION UL(X,Y)
  COMMON/O3/XT(40),YT(10),H(10),WP,B,DELX,YW
  COMMON/TY/T
  PI=3.141592654
  UL=2.0*T/PI/B*((0.5-X)*ALOG((X*X+Y*Y)/((1.0
1-X)**2+Y*Y))+2.0-2.0*Y*(ATAN(X/Y)+ATAN((1.0-X)/Y)))
  IF(X.GT.0..AND.X.LT.1.) UL=UL+(1./B*T*T*(3./PI/PI
1*(2.-2.*(X-.5)*ALOG(X/(1.-X)))**2-1./PI/PI*(ALOG(X/(1.-X
2)))**2-(1.-4.*(X-.5)**2)))
  RETURN
END
```

C
C
C

```
*****
```

THE FOLLOWING PACKAGE CALCULATES FUNCTIONS FOR BODY PROFILES, DERIVATIVE AND MODIFIED LINEAR PERTURBATION VELOCITY FOR INCOMPRESSIBLE AIRFOIL.

NOTE: - THE COMMON CARD /XYZ OF MAIN PROGRAM MUST BE CHANGED TO PRE COMMON CARD /XYZ USED IN THIS PACKAGE.

THIS FUNCTION CALCULATES AIRFOIL PROFILE
FUNCTION YY(X)

COMMON/TY/T,TBP,NB,B1,B2,B4,B6,B8,YX

B1=1.4245

B2=-0.93

B4=-1.756

B6=1.4215

B8=-0.5075

YY=0.0

IF(X.LT.0.0.OR.X.GT.1.0) RETURN

Y=B1*SQRT(X)+X*(B2+X*(B4+X*(B6+B8*X)))

YY=Y+T

RETURN

END

THIS FUNCTION CALCULATES THE DERIVATIVE OF AIRFOIL PROFILE
FUNCTION DY(X)

COMMON/TY/T,TBP,NB,B1,B2,B4,B6,B8,YX

DY=0.0

IF(X.LT.0.0.OR.X.GT.1.0) RETURN

DY=0.50*B1/SQRT(X)+B2+X*(2.*B4+X*(3.*B6+4.*B8*X))

DY=DY*T

RETURN

END

THIS FUNCTION CALCULATES MODIFIED LINEAR PERTURBATION VELOCITY
ON THE AIRFOIL

FUNCTION UB(X)

COMMON/Q3/S(40),P(10),H(10),B,DELX

COMMON/TY/T,TBP,NB,B1,B2,B4,B6,B8,YX

XQ=SQRT(ABS(X))

T2=ALOG(ABS(X/(1.-X)))

UH=B2*T2+2.*B4*(X*T2-1.)+3.*B6*(X*(X*T2-1.)-0.5)+4.*B8*(X*(X*(X*T2-1.)-0.5)-1./3.)

T1=B1/2./XQ*ALOG(ABS((1.+XQ)/(1.-XQ)))

IF(X.LT.0.0) T1=-B1/XQ*ATAN(1./XQ)

UB=TBP*(T1+UH)

IF(X.LT.0.0.OR.X.GT.1.0) RETURN

```

      OYX=OY(X)
      UB=(1.0+UB)/BORTCT,0+OYX*OYX/3/33-1.0
      RETURN
      END

```

```

C
C
C THIS FUNCTION CALCULATES MODIFIED HENRIE DIFFERENTIATION EQUATION
C ANYWHERE IN THE FIELD
      FUNCTION UB(X,Y)

```

```

      COMMON/YY/T,TBP,NB,B1,B2,B3,B5,B6,YX
      COMMON/O3/B(40),F(10),H(10),E,DEH,X
      TBP=T/O3*.141592654

```

```

      CHK=2.*B(1)+B

```

```

      IF(Y.LT,CHK) GO TO 20

```

```

      DEH=0.5*DEH/X

```

```

      IX=YI(X)

```

```

      SUM=FCT(X,Y,0.0)+4.0*FCT(X,Y,DEH)+FCT(X,Y,1.0)

```

```

      E2=DEH

```

```

      GO TO 1=2,NB

```

```

      E1=E2+DEH

```

```

      E2=E1+DEH

```

```

      SIMP=2.*FCT(X,Y,E1)+4.*FCT(X,Y,E2)

```

```

      SUM=SUM+SIMP

```

```

10 CONTINUE

```

```

      UM=SUM*DEH/3.

```

```

      UB=TBP*(UM+(YY(1.)-IX)*(X-1.)/(X-1.)**2+(Y)- (YI(0.0)-IX)+X/(X+X+
      Y+Y))/T

```

```

      RETURN

```

```

20 UB=OB(X)

```

```

      RETURN

```

```

      END

```

```

C
C
C THIS IS AUXILIARY FUNCTION IN COMPUTING UB(X,Y)
      FUNCTION FCT(X,Y,E)

```

```

      COMMON/YY/T,TBP,NB,B1,B2,B4,B6,B8,YX

```

```

      FCT=0.0

```

```

      DIF=ABS(X-E)

```

```

      IF(DIF.LT,0.0001) RETURN

```

```

      DFF=DIF*DIF

```

```

      DEN=DFF+Y*Y

```

```

      DNU=DEN-2.*Y*Y

```

```

      FCT=DNU/DEN/DEN*(YX-YY(E))

```

```

      RETURN

```

```

      END

```

```

*****

```

Date Slip ^A 62201

This image shows a single sheet of white paper with horizontal blue ruling lines. A vertical red margin line runs down the right side of the page. The paper appears to be from a notebook or a standard sheet of stationery. There are no markings, text, or drawings on the page.

CD 6.72.9

AE-1979-M-AGA-SUB